University of Zurich[UZH]

Zurich Open Repository and Archive
University of Zurich
University Library
Strickhofstrasse 39
CH-8057 Zurich
www.zora.uzh.ch

Year: 2020

Magnetic fields modulate metabolism and gut microbiome in correlation with Pgc-1 expression: Follow-up to an in vitro magnetic mitohormetic study

Tai, Yee Kit ; Ng, Charmaine ; Purnamawati, Kristy ; Yap, Jasmine Lye Yee ; Yin, Jocelyn Naixin ; Wong, Craig ; Patel, Bharati Kadamb ; Soong, Poh Loong ; Pelczar, Pawel ; Fröhlich, Jürg ; Beyer, Christian ; Fong, Charlene Hui Hua ; Ramanan, Sharanya ; Casarosa, Marco ; Cerrato, Carmine Pasquale ; Foo, Zi Ling ; Pannir Selvan, Rina Malathi ; Grishina, Elina ; Degirmenci, Ufuk ; Toh, Shi Jie ; Richards, Pete J ; Mirsaidi, Ali ; Wuertz-Kozak, Karin ; Chong, Suet Yen ; Ferguson, Stephen J ; Aguzzi, Adriano ; et al

Abstract: Exercise modulates metabolism and the gut microbiome. Brief exposure to low mT-range pulsing electromagnetic fields (PEMFs) was previously shown to accentuate in vitro myogenesis and mitochondriogenesis by activating a calcium-mitochondrial axis upstream of PGC-1 transcriptional upregulation, recapitulating a genetic response implicated in exercise-induced metabolic adaptations. We compared the effects of analogous PEMF exposure (1.5 mT, 10 min/week), with and without exercise, on systemic metabolism and gut microbiome in four groups of mice: (a) no intervention; (b) PEMF treatment; (c) exercise; (d) exercise and PEMF treatment. The combination of PEMFs and exercise for 6 weeks enhanced running performance and upregulated muscular and adipose Pgc-1 transcript levels, whereas exercise alone was incapable of elevating Pgc-1 levels. The gut microbiome Firmicutes/Bacteroidetes ratio decreased with exercise and PEMF exposure, alone or in combination, which has been associated in published studies with an increase in lean body mass. After 2 months, brief PEMF treatment alone increased Pgc-1 and mitohormetic gene expression and after >4 months PEMF treatment alone enhanced oxidative muscle expression, fatty acid oxidation, and reduced insulin levels. Hence, short-term PEMF treatment was sufficient to instigate PGC-1 -associated transcriptional cascades governing systemic mitohormetic adaptations, whereas longer-term PEMF treatment was capable of inducing related metabolic adaptations independently of exercise.

DOI: https://doi.org/10.1096/fj.201903005rr

Posted at the Zurich Open Repository and Archive, University of Zurich
ZORA URL: https://doi.org/10.5167/uzh-189281
Journal Article
Published Version

The following work is licensed under a Creative Commons: Attribution-NonCommercial 4.0 International (CC BY-NC 4.0) License.

Originally published at:

Tai, Yee Kit; Ng, Charmaine; Purnamawati, Kristy; Yap, Jasmine Lye Yee; Yin, Jocelyn Naixin; Wong, Craig; Patel, Bharati Kadamb; Soong, Poh Loong; Pelczar, Pawel; Fröhlich, Jürg; Beyer, Christian; Fong, Charlene Hui Hua; Ramanan, Sharanya; Casarosa, Marco; Cerrato, Carmine Pasquale; Foo, Zi Ling; Pannir Selvan, Rina Malathi; Grishina, Elina; Degirmenci, Ufuk; Toh, Shi Jie; Richards, Pete J; Mirsaidi, Ali; Wuertz-Kozak, Karin; Chong, Suet Yen; Ferguson, Stephen J; Aguzzi, Adriano; et al (2020). Magnetic fields modulate metabolism and gut microbiome in correlation with Pgc-1 expression: Follow-up to an in vitro magnetic mitohormetic study. FASEB Journal, 34(8):11143-11167.
DOI: https://doi.org/10.1096/fj.201903005rr

Received: 28 November 2019 | Revised: 7 June 2020 | Accepted: 15 June 2020

DOI: 10.1096/fj.201903005RR

RESEARCH ARTICLE

THE FASEB JOURNAL

Magnetic fields modulate metabolism and gut microbiome in correlation with *Pgc-1α* expression: Follow-up to an in vitro magnetic mitohormetic study

Yee Kit Tai[1,2] | Charmaine Ng[1] | Kristy Purnamawati[1,2] | Jasmine Lye Yee Yap[1,2] | Jocelyn Naixin Yin[1,2] | Craig Wong[1,2] | Bharati Kadamb Patel[1] | Poh Loong Soong[1,2] | Pawel Pelczar[3,4] | Jürg Fröhlich[5] | Christian Beyer[6] | Charlene Hui Hua Fong[1,2] | Sharanya Ramanan[1,2] | Marco Casarosa[7,8] | Carmine Pasquale Cerrato[9] | Zi Ling Foo[1,2] | Rina Malathi Pannir Selvan[1,2] | Elina Grishina[1,2] | Ufuk Degirmenci[10] | Shi Jie Toh[1,2] | Pete J. Richards[11] | Ali Mirsaidi[11] | Karin Wuertz-Kozak[11,12,13] | Suet Yen Chong[1,13] | Stephen J. Ferguson[10,11] | Adriano Aguzzi[14] | Monica Monici[15] | Lei Sun[16] | Chester L. Drum[1,13] | Jiong-Wei Wang[1,13,17] | Alfredo Franco-Obregón[1,2,10,17,18]

[1]Department of Surgery, Yong Loo Lin School of Medicine, National University of Singapore, Singapore, Singapore

[2]Biolonic Currents Electromagnetic Pulsing Systems Laboratory, BICEPS, National University of Singapore, Singapore, Singapore

[3]Centre for Transgenic Models, University of Basel, Basel, Switzerland

[4]Institute of Laboratory Animal Science, University of Zürich, Zürich, Switzerland

[5]Fields at Work GmbH, Zürich, Switzerland

[6]Centre Suisse d'électronique et de microtechnique, CSEM SA, Neuchatel, Switzerland

[7]Department of Experimental and Clinical Biomedical Sciences "Mario Serio", University of Florence, Florence, Italy

[8]Institute for Biomechanics, ETH Zürich, Zürich, Switzerland

[9]Institute of Environmental Medicine, Karolinska Institutet, Stockholm, Sweden

[10]Institute of Molecular and Cell Biology, A*STAR, Singapore, Singapore

[11]Competence Center for Applied Biotechnology and Molecular Medicine, University of Zürich, Zürich, Switzerland

Abbreviations: +E, exercise; +P, pulsed electromagnetic field treatment; –E, no exercise; –P, no pulsed electromagnetic field treatment; ADIPOQ, adiponectin, C1Q and collagen domain containing; B2M, beta-2-microglobulin; BAT, brown adipose tissue; CEBP–α, CCAAT/enhancer-binding protein α; COX7a1, cytochrome c oxidase polypeptide 7A1; CPT1B, carnitine palmitoyltransferase 1B; CR, caloric restriction; DIO2, Iodothyronine deiodinase 2; EDL, extensor digitorum longus; ELOVL3, elongation of very long fatty acids protein 3; FASN, fatty acid synthase; FAT/CD36, Fatty acid translocase, Cluster of differentiation 36; FMT, fecal microbiota transplant; FNDC5, fibronectin type III domain-containing protein 5; GASP1, G-protein coupled receptor-associated sorting protein 1; GRASP1, G-protein coupled receptor-associated sorting protein 1; GXTm, graded maximal exercise test; IACUC, Institutional Animal Care and Use Committee; IGF1, insulin-like growth factor 1; IL-6, interleukin-6; KEGG, Kyoto Encyclopedia of Genes and Genomes; LEP, leptin; LEfSe, linear discriminant analysis effect size; MCSs, mesenchymal stem cells; MEF2C, myocyte-specific enhancer factor 2; MRPS12, mitochondrial ribosomal protein S12; MYOG, myogenin; NAMPT, nicotinamide phosphoribosyltransferase; NFAT, nuclear factor of activated T-cells; NQO1, NAD(P)H [quinone] dehydrogenase 1; NRF1, nuclear respiratory factor 1; NRF2, nuclear respiratory factor 2; OTUs, operational taxonomic units; PCO, principal coordinate analysis; PEMF, pulsed electromagnetic field; PERMANOVA, permutational multivariate analysis of variance; PGC–1α, peroxisome-proliferator activated receptor γ coactivator 1 α; PICRUSt, phylogenetic investigation of communities by reconstruction of unobserved states; PPARGC1α, peroxisome proliferator-activated receptor γ coactivator 1 α; PRDM16, PR domain containing 16; RER, respiratory exchange ratio; RPL23, ribosomal protein L23; SCFA, short-chain fatty acids; SIRT1, NAD-dependent deacetylase sirtuin-1; SOD2, superoxide dismutase 2; SRA, sequence read archive; TFAM, transcription factor A, mitochondrial; TFEB, transcription Factor EB; TRP, transient receptor potential; TRPC1, transient receptor potential channel 1; TRIM55, tripartite motif-containing protein 55; VEGFA, vascular endothelial growth factor A; UCP1, uncoupling protein 1; WAT, white adipose tissue.

This is an open access article under the terms of the Creative Commons Attribution-NonCommercial License, which permits use, distribution and reproduction in any medium, provided the original work is properly cited and is not used for commercial purposes.

© 2020 The Authors. *The FASEB Journal* published by Wiley Periodicals LLC on behalf of Federation of American Societies for Experimental Biology

[12]Department of Biomedical Engineering, Rochester Institute of Technology (RIT), Rochester, NY, USA

[13]Cardiovascular Research Institute (CVRI), National University Heart Centre Singapore (NUHCS), Singapore, Singapore

[14]Institut für Neuropathologie, Universitätsspital Zürich, Zürich, Switzerland

[15]ASAcampus JL, ASA Res. Div. - Dept. of Experimental and Clinical Biomedical Sciences "Mario Serio", University of Florence, Florence, Italy

[16]DUKE-NUS Graduate Medical School Singapore, Singapore, Singapore

[17]Department of Physiology, Yong Loo Lin School of Medicine, National University of Singapore, Singapore, Singapore

[18]Institute for Health Innovation & Technology, iHealthtech, National University of Singapore, Singapore, Singapore

Correspondence
Alfredo Franco-Obregón, Department of Surgery, Yong Loo Lin School of Medicine, National University of Singapore, NUHS Tower Block Level 8, 1E Kent Ridge Road, Singapore 119228, Singapore.
Email: suraf@nus.edu.sg

Funding information
Lee Foundation, Grant/Award Number: N-176-000-045-001; Grant/Award Number: Institute for Health Innovation & Technology, iHealthtech, National University of Singapore: R-176-000-243-731 Ministry of Education Academic Research Fund, MOE2018-T2-2-158: R-722-000-018-112; European Space Agency (ESA), Grant/Award Number: 4000113883; Fondation Suisse de Recherche sur les Maladies Musculaires

Abstract

Exercise modulates metabolism and the gut microbiome. Brief exposure to low mT-range pulsing electromagnetic fields (PEMFs) was previously shown to accentuate in vitro myogenesis and mitochondriogenesis by activating a calcium-mitochondrial axis upstream of PGC-1α transcriptional upregulation, recapitulating a genetic response implicated in exercise-induced metabolic adaptations. We compared the effects of analogous PEMF exposure (1.5 mT, 10 min/week), with and without exercise, on systemic metabolism and gut microbiome in four groups of mice: (a) no intervention; (b) PEMF treatment; (c) exercise; (d) exercise and PEMF treatment. The combination of PEMFs and exercise for 6 weeks enhanced running performance and upregulated muscular and adipose *Pgc-1α* transcript levels, whereas exercise alone was incapable of elevating *Pgc-1α* levels. The gut microbiome *Firmicutes*/*Bacteroidetes* ratio decreased with exercise and PEMF exposure, alone or in combination, which has been associated in published studies with an increase in lean body mass. After 2 months, brief PEMF treatment alone increased *Pgc-1α* and mitohormetic gene expression and after >4 months PEMF treatment alone enhanced oxidative muscle expression, fatty acid oxidation, and reduced insulin levels. Hence, short-term PEMF treatment was sufficient to instigate PGC-1α-associated transcriptional cascades governing systemic mitohormetic adaptations, whereas longer-term PEMF treatment was capable of inducing related metabolic adaptations independently of exercise.

KEYWORDS
brown adipose, mitochondria, muscle, PEMF, white adipose

1 | INTRODUCTION

The gut microbiome is a dynamic and complex microbial community hosted by humans in mutual benefit. The microbiome responds to alterations in lifestyle[1,2] by modulating metabolism,[3,4] immunity,[5] and overall health.[6] Physiological status is thus established through a delicate balance of host-gut microbiota interactions that are influenced by host genetics and age yet, susceptible to perturbations in diet, medications, physical activity as well as other environmental factors.[6,7] Previous studies have elucidated evidence of bidirectional communication between residing microbial communities and the host and have sought to understand its underlying mechanisms.[8-10]

The subtle modulation of host metabolism by the gut microbiome was elegantly demonstrated in a recent study whereby functional beiging (mitochondrial uncoupled respiration) of the inguinal subcutaneous and perigonadal visceral adipose deposits of obese mice was promoted by depletion of the adiposity-associated gut microbiota.[10] Caloric restriction (CR) also improves metabolism[11] and can be transmitted to recipient mice with transplantation of CR-conditioned microbiome. Whereas, fecal microbiota transplant (FMT) from CR mice into obese mice reversed hepatic lipid accumulation,[9] FMT of CR-microbiota into germ-free mice promoted fat browning.[8] The microbiome is thus capable of adopting both negative and positive aspects of host metabolism, that moreover, are subject to environmental modulation. The metabolic attributes of CR are associated with improvements in muscular mitochondrial function mediated by PGC-1α.[11] Notably, key metabolites produced by the microbial gut communities

have been shown to act as signaling/substrate molecules that regulate mitochondrial-dependent systemic energy balance.[12] Hence, evidence suggests that the mitochondria and microbiome mutually sustain the function of the other, which, in turn, would go toward establishing systemic metabolic balance.

Skeletal muscle hosts a large activatable pool of mitochondria that impacts systemic metabolism and fatty acid oxidation.[13-15] In a retrograde manner, germ-free mice lacking a microbiota exhibited muscle atrophy and reduced mitochondrial function.[16] FMT from normal mice into these germ-free mice recuperated both skeletal muscle mass and mitochondrial function. Notably, *Pgc-1α* and *Igf-1* transcript levels were reduced in skeletal muscle from these germ-free mice and recovered upon FMT from normal mice. Recently, the short-chain fatty acids (SCFAs), microbiome fermentation metabolites, have been found to act as agonists for PGC-1α upstream of enhanced mitochondriogenesis and free fatty acid oxidation.[17-19] The proper functioning of this microbiome-mitochondria axis should thus support muscle energetics as well as be accentuated by exercise.[18]

Via such a mechanism exercise would prime the gut microbiome toward metabolic improvement.[2,20-22] Oxidative muscle would be particularly relevant in this respect as it exhibits elevated mitochondrial content[23] as well as predilections for fatty acid oxidation and in supporting insulin-sensitivity.[24] Exercise promotes oxidative muscle development, whereas inactivity results in oxidative muscle atrophy. Oxidative fibers are also characterized by elevated resting calcium levels that diminish with inactivity and precede a reversal in oxidative character.[25] In this manner, the calcium-permeable channel, Transient Receptor Potential Subfamily C Member 1 (TRPC1), is mechanistically linked to oxidative muscle development.[26,27] TRPC1 expression is highest in oxidative muscle fibers[28] and wanes with disuse.[26] Likewise, silencing TRPC1 expression results in oxidative muscle loss.[26] Calcium entry via TRPC1 activates the nuclear factor of activated T-cells (NFAT)[26,29] that, in turn, sustains TRPC1 expression[26,30] as well as those of PGC-1α and oxidative muscle.[23] Accordingly, NFAT and TRPC1 levels decrease upon mechanical unloading and revert upon reloading,[26] mirroring decreases and increases of oxidative muscle expression, respectively. Ample evidence thus supports cooperative roles for TRPC1, NFAT, and PGC-1α in oxidative muscle functional capacity and via inference, to microbiome composition via its elevated mitochondrial respiratory capacity.

In response to mitochondrial activation via exercise, skeletal muscle produces and releases a myriad of cytokines, collectively known as myokines,[31] that promote, among other responses, the beiging of white adipose tissue (WAT).[32,33] In turn, "beiged" adipose releases adipokines (aka batokines), some of which are in common with the myokine pool, to further promote brown adipose recruitment.[34] Therefore, muscle mitochondrial activation initiates a cytokine cascade that ultimately grows to encompass batokines for the reinforcement of systemic metabolic balance. Moreover, adipose beiging can be transmitted with FMT from fasting-induced beiged into microbiome-depleted mice,[35] reflecting a form of microbiome-muscle/adipose interdependency that could potentially be exploited clinically, provided the correct intervention were available.

Motivated by previous studies underscoring the homeostatic role that muscle mitochondrial activation plays over systemic metabolism and gut microbiome, we examined whether muscle mitochondrial stimulation employing a novel noninvasive magnetic paradigm[36] might elicit similar responses to exercise. We have previously demonstrated that brief (10 minutes) exposures to low amplitude (≤2 mT) pulsing electromagnetic fields (PEMFs) applied to myoblasts or mesenchymal stem cells (MSCs) were necessary and sufficient to enhance in vitro myogenesis[36] or chondrogenesis,[37] respectively. Importantly, brief PEMF treatment was shown to promote in vitro myogenesis by activating a TRPC1-mitochondrial axis upstream of enhanced *Pgc-1α* expression and mitochondriogenesis.[36] Here, we show that this same magnetic stimulation paradigm also proved relevant for the in vivo scenario. Mice exposed to PEMFs (10 min/week) for a few months showed increases in oxidative muscle development, enhanced fatty acid oxidation, and improved insulin-sensitivity. Moreover, 6 weeks of analogous PEMF exposure was sufficient to accentuate the metabolic consequences of exercise on muscle and adipose tissues, enhanced running performance as well as produced unique shifts in gut microbiome communities that are associated with key metabolic functions. All effects were correlated with elevated *Pgc-1α* expression levels in muscle and adipose tissues in accordance with the installation of systemic mitohormetic adaptations.

2 | MATERIALS AND METHODS

2.1 | Animal studies

2.1.1 | Husbandry and institutional clearances

Long-term study

The mouse study was approved by the veterinary authority of the canton Zurich and conducted under license no 156/2011. All the mice were housed in socially compatible groups under a 12 hours/12 hours light/dark cycle with food and water ad libitum. Experimental groups (n = 6) of female C56BL/6J mice (Jackson labs) were subjected

to a 6-month regime of PEMF exposure commencing at 8 weeks of age.

Short-term study

This protocol was approved by the Institutional Animal Care and Use Committee (IACUC) of the National University of Singapore, and followed the Guide for the Care and Use of Laboratory Animals. All experiments were performed on 8-week-old, female C57BL/6NTac mice, housed individually, with 12 hours/12 hours light/dark cycles and maintained on a standard chow diet.

2.1.2 | PEMF exposure and exercise regimes

The PEMF device used in this study has been previously described.[36] Succinctly, exposure to 1.5 mT amplitude PEMFs for 10 minutes applied once was best suited to promote in vitro myogenesis. In the present study, an analogous PEMF exposure paradigm was employed on behaving mice. Specifically, C56BL/6J mice were exposed once per week for a duration of 10 minutes at an amplitude between 1 and 1.5 mT, unless otherwise indicated. For the short-term exercise study PEMF exposure at an amplitude of 1.5 mT was applied to C57BL/6NTac mice once per week on Sundays for 10 minutes. Exhaustive running was conducted thrice per week, commencing on the following Mondays, Wednesdays, and Fridays for six consecutive weeks. Mice were sacrificed on week 7.

We adapted the Graded Maximal Exercise Test (GXTm) protocol with modification: instead of electrical grid shock, we utilized auditory stress to encourage treadmill running—paper towels were placed in between the inactivated shock grids such that they would interact with the rotating belt of the treadmill and create noise (Columbus Instruments, Ohio, USA) while the treadmill was in operation.[38] We found that this noise was sufficient to encourage the mice to continue running before they reached exhaustion.

Prior to the start of the study, mice were acclimatized to the treadmill using two walking sessions where they were put on a stationary treadmill for 5 minutes, followed by 10 minutes of walking at 6 m/min. The exercise regime was as follows (speed, duration, grade)—(0 m/min, 3 minutes, 0°), (6 m/min, 2 minutes, 0°), (9 m/min, 2 minutes, 5°), (12 m/min, 2 minutes, 10°), (15 m/min, 2 minutes, 15°), (18, 21, 23, 24 m/min, 1 minute, 15°), and (+1 m/min, each 1 minute thereafter, 15°) until exhaustion. The maximal speed achieved in every running session was recorded. We defined exhaustion as the point at which mice rested onthe paper towel for 30 seconds with no further attempt to get back on the treadmill, despite persistent auditory stimulation.

2.1.3 | Indirect calorimetry

Indirect calorimetry measurements were performed with the PhenoMaster (TSE Systems) according to the manufacturer's guidelines and protocols. O_2 and CO_2 levels were measured for 60 seconds every 13 minutes continuously with PhenoMaster (TSE Systems). Energy expenditure was calculated according to the manufacturer's guidelines (PhenoMaster Software, TSE System). The respiratory quotient was estimated by calculating the ratio of CO_2 production to O_2 consumption. Animals were single caged and acclimated to the metabolic cages for 48 hours before metabolic recording.

2.1.4 | Plasma biochemistry analysis

For long-term PEMF studies (>8 weeks), mice were fasted for 6 hours before sacrifice. Blood samples were obtained via cardiac puncture, and plasma was collected after centrifugation for 15 minutes at 3000 rpm at 4°C. Cholesterol and triglycerides were measured by enzymatic tests (Roche Diagnostics). Plasma insulin levels were measured using mouse/rat insulin kit (Meso Scale Discovery) as per manufacturer's instructions. Plasma samples for measuring fasting/refeeding NEFAs were obtained after 12 hours of fasting and 4 hours of refeeding, using NEFAs kit (WAKO).

For the short-term studies, plasma was centrifuged for 10 minutes at 10 200 rpm at 4°C. For quantitative determination of plasma IL-6, insulin, leptin, adiponectin, and VEGFA evaluated by magnetic bead-based multiplex assay was performed using Bio-Plex Pro Mouse Cytokine 23-Plex Assay and Bio-Plex Pro Mouse Diabetes Adiponectin Assay (Bio-Rad, USA). The results were read using Bio-Rad 200 System microplate photometer (Bio-Rad, USA) and read using Bio-Plex Manager software (Bio-Rad, USA). IL-6, insulin, leptin, and adiponectin concentrations were determined using a standard curve (determined dynamic range of 0.74-12 053 pg/mL, 93.4-47 815 pg/mL, 17.1-69 900 pg/mL, and 38.0-62 043 pg/mL, respectively) according to manufacturer's instructions.

2.1.5 | Muscle histology

Mice were euthanized by CO_2 inhalation and the gastrocnemius and soleus muscles dissected, fixed with 4% of formaldehyde, dehydrated and embedded in paraffin for oxidative (fast) or glycolytic (fast) muscle fiber detection. The paraffin sections were stained with the NCL-MHCf monoclonal antibody (Novocastra) to detect slow myosin heavy chain. Images were analyzed using ImageJ (public domain, National Institutes of Health, USA).

2.1.6 | Adipose tissue isolation

Following CO_2 euthanization, interscapular brown and subcutaneous white inguinal adipose samples were harvested and immediately snap frozen in liquid nitrogen. For genetic analysis, frozen samples were pulverized and their total RNAs extracted for downstream quantitative PCR experiment.

2.1.7 | Primary adipocyte isolation and adipocyte differentiation

Inguinal adipose harvested from 3- to 4-week-old C57BL/6J mice were washed, minced, and then, digested for 25 minutes at 37°C with brief intermittent vortex every 5 minutes in collagenase (0.2%, Sigma). Digestion was stopped with DMEM and dissociated cells were filtered through a 100 mm strainer. Isolated SVF cells were spun down by centrifugation at 1000 rpm for 5 minutes, and then, resuspended for plating in DMEM containing 10% of fetal bovine serum (FBS, Invitrogen), 50 units/mL of penicillin, 50 mg/mL of streptomycin, and 10 mg/mL of gentamicin (Invitrogen) at 10% CO_2 at 37°C. For adipocyte differentiation, confluent cultures were exposed to an adipogenic cocktail supplemented with dexamethasone (0.5 mM, Sigma), insulin (0.85 mM, Sigma), isobutylmethylxanthine (250 mM, Sigma), rosiglitazone (1 mM, Sigma) in DMEM containing 10% of FBS for 48 hours. Otherwise, cells were maintained in DMEM containing 10% of FBS.

2.2 | Gut microbiome profiles

2.2.1 | Microbiome sampling of stool

At termination, mice were euthanized by CO_2 asphyxiation and their ceca, and wet fecal matter contained therein were immediately snap frozen in liquid nitrogen and stored at –80°C until further analysis. Cecal and fecal samples were thawed, weighed, and total bacterial DNA was extracted using the DNeasy PowerSoil Kit (Qiagen, Hilden, Germany) according to manufacturer's instructions. Total yield and purity of DNA were measured using a NanoDrop One Spectrophotometer (Thermo Scientific, Delaware, USA).

2.2.2 | Microbiome profiling of stool samples

Three mice were selected from each treatment group: No exercise and no PEMF treatment (–E/–P); No exercise plus PEMF treatment (–E/+P); Exercise and no PEMF treatment (+E/–P); Exercise plus PEMF treatment (+E/+P) to determine microbial community composition of cecal and fecal samples of mice belonging to the different treatment groups (Figure S1). This was achieved by 16S rRNA gene amplicon sequencing targeting the V4 region of bacterial 16S rRNA genes using 515F (5′-GTGCCAGCMGCCGCGG-3′) and 907R (5′-CCGTCAATTCMTTTRAGTTT-3′) primers. Samples were sequencing on the Illumina MiSeq platform at the Argonne sequencing core (Chicago, USA). Sequenced data were processed using the QIIME[39] pipeline where reads were trimmed, quality checked, and aligned to the Green Genes database, clustered at 97% similarity into Operational taxonomic units (OTUs) and annotated against the SILVA ribosomal RNA database. Sequence reads were deposited into the NCBI Sequence read archive (SRA) under the BioProject number PRJNA482925. Linear discriminant analysis effect size (LEfSe), was used to determine statistically significant OTUs which contributed to differences between the treatment groups.[40]

2.2.3 | Predictive pathways of the gut microbiota

A.biome file was created using QIIME and analyzed using the bioinformatics software PICRUSt to predict the functional composition of the gut microbial community from the 16S rRNA gene profile and LefSe was used to identify statistically significant biological pathways which defined each treatment group.[41]

2.3 | Muscle and tissue gene expression profiles

2.3.1 | qPCR

Quantitative Reverse-Transcription Polymerase Chain Reaction (RT-qPCR) was carried out on muscle and adipose tissue samples with TaqMan or SYBR green-based detection workflow. The list of qPCR primers can be found in Table 1.

2.3.2 | Mouse muscle samples, TaqMan-based workflow

The soleus and extensor digitorum longus (EDL) muscles of mice were harvested at study termination, washed in PBS, snap frozen in liquid nitrogen, and stored at –80°C. Total RNAs were then extracted by TRIzol reagent (Thermo Scientific) and quality assessed using the Agilent 2200 Tape station system and

TABLE 1 List of qPCR Primers in muscle and adipose tissues

Gene	Forward primer sequence (5′ … 3′)	Reverse primer sequence (5′ … 3′)
Adipose tissue		
Rpl23	TGTGAAGGGAATCAAGGGA	TGTTTACTATGACCCCTGCG
Lep	GAGACCCCTGTGTCGGTTC	CTGCGTGTGTGAAATGTCATTG
Cox7a1	CAGCGTCATGGTCAGTCTGT	AGAAAACCGTGTGGCAGAGA
Pgc-1α	AGCCGTACCACTGACAACGAG	GCTGCATGGTTCTGAGTGCTAAG
Prdm16	CAGCACGGTGAAGCCATTC	GCGTGCATCCGCTTGTG
Elovl3	TCCGCGTTCTCATGTAGGTCT	GGACCTGATGCAACCCTATGA
AdipoQ	GCACTGGCAAGTTCTACTGCAA	GTAGGTGAAGAGAACGGCCTTGT
Dio2	CAGTGTGGTGCACGTCTCCAATC	TGAACCAAAGTTGACCACCAG
Fasn	GGAGGTGGTGATAGCCGGTAT	TGGGTAATCCATAGAGCCCAG
Ucp1	ACTGCCACACCTCCAGTCATT	CTTTGCCTCACTCAGGATTGG
Glut4	CTGTCGCTGGTTTCTCCAACT	CCCATAGCATCCGCAACATA
Irs1	CGATGGCTTCTCAGACGTG	CAGCCCGCTTGTTGATGTG
Cebp-α	TGCGCAAGAGCCGAGATAAA	CCTTCTGTTGCGTCTCCACG
Nampt	TGGGGTGAAGACCTGAGACA	CTTCTGTAGCAAAGCGCCAC
Muscle tissue		
B2m	GATGTCAGATATGTCCTTCAGCA	TCACATGTCTCGATCCCAGT
Pgc-1α	CCCTGCCATTGTTAAGACC	TGCTGCTGTTCCTGTTTTC
Nampt	AGACTGCTGGCATAGGGGCA	CCGTTATGGTACTGTGCTCTGCT
Sirt1	TGACCGATGGACTCCTCACT	ACAAAAGTATATGGACCTATCCGC
Cpt1b	GGCACCTCTGGGAGTTTGTCC	GGCAACGTGGTGTTTGGCTC
Nrf1	AATGACCCACGCTCAGCTTC	GCTTGCAGCTTTCTTTCCCC
Nrf2	TGAAGCTCAGCTCGCATTGA	TGCTCCAGCTCGACAATGTT
Tfeb	TGTCTAGCAGCCACCTGAAC	GCTCTGCTCTCAGCATCTGT
Tfam	GCTGAAGTTGGACGAAGTGA	CCCAATGACAACTCCGTCTT
Nqo1	AAACGTCTGGAAACCGTCTG	TTCTGCTCCTCTTGAACTTCC
Pparα	GCAACCATCCAGATGACACC	TCTCTTGCAACAGTGGGTGC
Sod2	TCTGTGGGAGTCCAAGGT TC	TAAGGCCTGTTGTTCCTTGC
Gene	**Company**	**Cat no**
Muscle tissue (TaqMan probe)		
B2m	Applied Biosystems	Mm00437762_m1
Mef2c		Mm01340842_m1
Vegf-a		Mm00437306_m1
Grasp1		Mm01302078_m1
Fndc5		Mm01181543_m1
Trim55		Mm01292969_m1
Mrps12	Thermo Scientific	Mm00488728_m1
Pgc-1α		Mm01208835_m1
Igf1		Mm00439560_m1
Cd36		Mm00432398_m1
Trpc1		Mm00441973_m1
Mef2c		Mm01340842_m1
Myog		Mm00446194_m1

the Agilent Bioanalyzer 2100 (Agilent, Waldbronn, Germany). Following treatment with TURBO DNase (Thermo Scientific), equal amounts of RNA from each animal per treatment group (n = 8) were combined and reverse transcribed using Superscript II (Thermo Scientific). Alternatively, when sufficient total RNAs were obtained from each animal, they were reverse transcribed as separate biological replicates. Quantification of mRNA expression levels in each sample was performed with TaqMan Gene Expression Assays (Thermo Scientific) using the StepOnePlus Real-Time PCR System (Life Technologies). All values were normalized to *Mrps12* (Mm00488728_m1) and presented as fold-changes. Each 10 μL reaction consisted of 1X TaqMan Fast Universal PCR Master Mix (Life Technologies), 1X TaqMan Gene Expression Assay and 10 ng cDNA. All reactions were performed in fast optical 96-well reaction plates (Life Technologies) at 95°C for 20 seconds and 40 cycles of 95°C for 1 second and 60°C for 20 seconds.

2.3.3 | Mouse muscle samples, SYBR green-based workflow

Tissue harvest, preservation, and total RNAs extraction were as in TaqMan-based workflow above. Reverse transcription of total RNAs was carried out using the iScript cDNA synthesis kit (Bio-Rad) and gene expression levels were analyzed with Sso advanced Universal SYBR Green Supermix (Bio-Rad). Each 10 μL reaction consisted of 1X SYBR green mix, 100 - 150 nM of forward and reverse primers, and 10 ng cDNA. Amplification parameters were: 1 cycle of enzyme activation step (1x, 95°C, 5 minutes), 40 cycles of denaturation (95°C, 10 seconds), and annealing/extension (primer-specific temperature 55°C-60°C, 30 seconds) steps, followed by 1 cycle of melt curve(95°C for 15 seconds, annealing temperature for 1 minute and ramp up to 95°C in increments of 0.5°C) and cooling at 10°C. *B2m* was amplified at 55°C, *Pgc-1α* at 57°C, *Sirt1* at 58°C, and all other primers at 60°C. All transcripts were normalized to *B2m*.

2.3.4 | Mouse adipose samples, SYBR green-based workflow

Mouse adipose samples were homogenized using Magna Lyser machine and ZIRCONIA beads. Total RNA was isolated using easy-BLUE (TM). Total RNA extraction and clean-up was conducted using QIAGEN RNeasy Mini kit. cDNA was generated using M-MLV reverse transcriptase kit and random hexamers (both from Invitrogen). Real-time PCR was performed using Applied Biosystems ViiA7 and SensiFAST SYBR Hi-ROX kit (Bioline). All transcripts were normalized to *Rpl23*. PCR conditions used were 50°C for 2 minutes, 95°C for 10 minutes, followed by 40 cycles of 95°C for 15 seconds and 60°C for 1 minute. Experiments were done with at least five independent samples and three technical replicates per sample. Relative gene expression was presented as ΔΔCt.

2.4 | Statistical analysis

The statistical software package PRIMER–E version 7[42] was used to analyze similarities in cecal and fecal microbiota composition between different treatment groups. Briefly, the OTU abundance data generated by QIIME was normalized using a log (x + 1) transformation and the distance matrices between treatment groups were calculated using a Bray-Curtis analysis and presented as a Principal Coordinate Analysis (PCO). A permutational multivariate analysis of variance (PERMANOVA) test was used to verify if microbial compositions between the treatment groups were significant, and a pairwise PERMANOVA test was used to validate difference between two groups.

For the analysis of gene expression, a two-way ANOVA test was used to determine significant differences in muscle and adipose tissues in response to distinct interventions. Statistical estimation plots were also applied to our short-term (6 weeks) mouse study to estimate effect size and uncertainty.[43] The Δ values in these plots represent the difference of means between the control and experimental group where the effect size is denoted by the black dot in the Δ value panels and the uncertainty of the estimate is shown by the gray-colored violin plot. The black line passing through the black dot denotes 95% confidence interval of the estimates. If the line does not cross zero (gray horizontal line), it is an equivalent finding to having a P value of .05, or better. Additionally, a pairwise Student's t test was conducted for each experimental condition relative to its correspondent control scenario (0 mT, non-exercised; (–E/–P) and is indicated in each plot by red ** or * to denote $P < .01$ and $< .05$, respectively.

3 | RESULTS

3.1 | Brief, weekly PEMF exposure enhances oxidative muscle development in mice

We previously reported that extremely low frequency and low amplitude PEMFs applied once for 10 minutes promoted in vitro myogenesis by activating a TRPC-mitochondrial axis upstream of PGC-1α activation,[36] the same genetic response previously implicated in exercise-enhanced oxidative muscle development.[23-30] Here, we tested the efficacy of an analogous PEMF exposure paradigm on mice. Mice were exposed to either 0 (sham controls), 0.5, 1, or 2 mT amplitude PEMFs for 10 minutes per week for 6 months, followed

by examination of the Soleus, a predominantly oxidative muscle. The cross-sectional area of oxidative muscle fibers decreased in PEMF-treated mice (Figure 1A), representing a known metabolic adaptation[44] aimed at facilitating oxygen uptake into oxidative fibers with heightened mitochondrial respiratory capacities and linked to the expressions of PGC-1α[44] and myogenin.[45] This effect became apparent at 1 mT applied once, rather than thrice, weekly (Supplemental Figure S2), recapitulating a similar sensitivity as delineated in vitro.[36] By contrast, the cross-sectional area of glycolytic fibers was unchanged by PEMF treatment (Figure 1A, inset). These results demonstrate that brief weekly PEMF treatment promotes functional adaptations in oxidative muscle in vivo. From here onward, all data relating to PEMF exposure will be depicted in blue and their correspondent control scenarios (0 mT) in red.

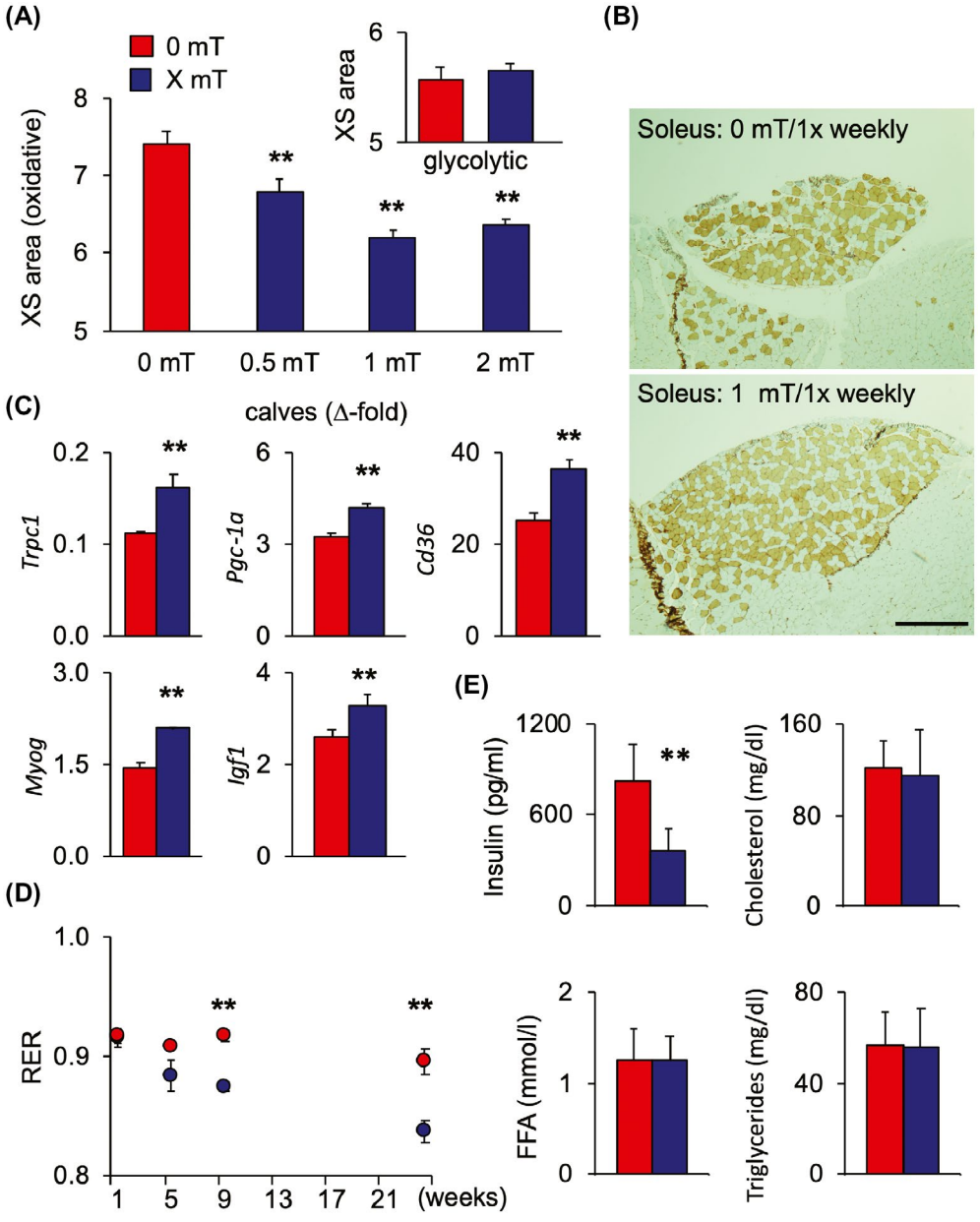

FIGURE 1 Weekly PEMF exposure enhances oxidative muscle capacity in mice. A, Cross-sectional area of oxidative muscle fibers following PEMF treatment; 0 mT (n = 279 fibers), 0.5 mT (n = 240), 1 mT (n = 635), 2 mT (n = 954) (see Supplemental Figure S2). Inset) Glycolytic fibers cross-sectional area from exposed (blue; n = 312) or control (red; n = 178) mice; (a.u. ($\times 10^3$)). B, Solei muscles stained for slow myosin heavy chain. Scale bar = 500 μm. C, NFAT-regulated gene expression from calf musculature of mice exposed once/week. D, Indirect calometric measurement of respiratory exchange ratio (RER). E, Serum markers after 4 months of weekly PEMF exposure (also see Figure S7). All PEMF exposures were for 10 minutes. Panels A, B, D represent data generated from female mouse cohorts of 6 mice/condition. Panels C and E represent data generated from 8 to 16 female mice/condition, respectively. PEMF treatment (2 mT) was for 4 (C-E) or 6 months (A,B) without additional exercise. ** and *$P < .01$ and $< .05$, respectively, wrt correspondent 0 mT.

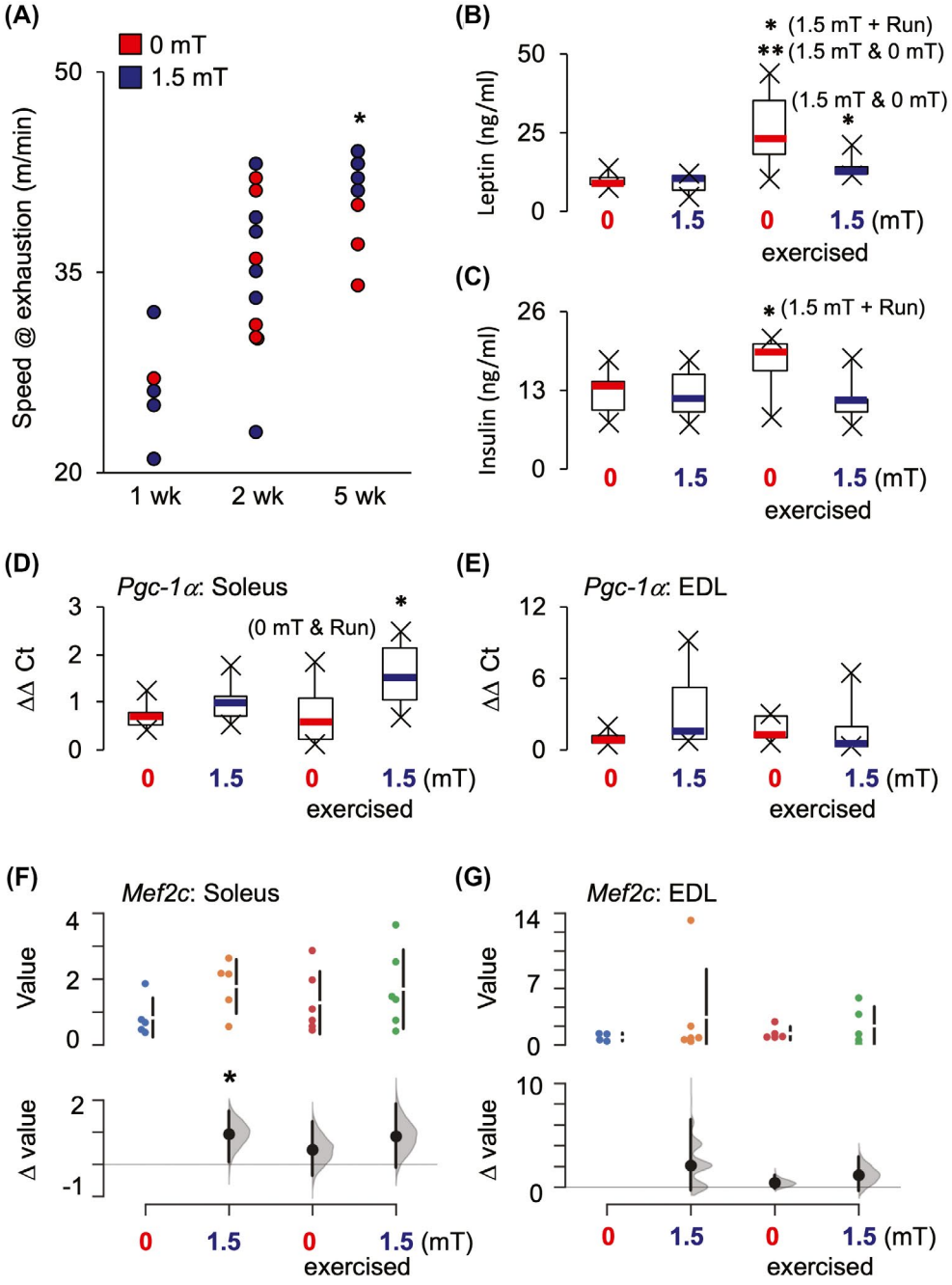

FIGURE 2 PEMF treatment accentuates the effects of weekly exercise in mice. A, Running performance in mice ran to exhaustion thrice/week and exposed to PEMFs (1.5 mT) once/week. Shown is the running performance during the third trial of each indicated week (see Methods). Serum leptin (B) and insulin (C) levels of the indicated experimental groups after 6 weeks of treatment. *Pgc-1α* transcript levels in our four indicated intervention groups in the Soleus (D) and EDL (E) muscles analyzed by two-way ANOVA (see Table 2 for details). Statistical estimation plots[43] for *Mef2c* for the Solei (F) and EDL muscles (G) under our four experimental conditions. The Δ values represent the difference of means between the control and experimental groups, the effect size is denoted by a black dot in the Δ value panels and the uncertainty of the estimate is shown by the gray-colored violin plot. The black line passing through the black dot denotes 95% confidence interval of the estimates. If the line does not cross zero (gray horizontal line), it is an equivalent finding to having *P* value .05, or better (also see Figure S3). All PEMF exposures were for 10 minutes. All means are derived from six female mice/condition. ** and *$P < .01$ and $< .05$, respectively, relative to the indicated experimental group.

Transcripts for the NFAT-regulated genes, *Trp1*,[30] *Pgc-1α*,[23,46] and *Myog* (myogenin)[47] were previously shown to be upregulated by PEMF exposure promoting in vitro myogenesis.[36] Analogously, transcripts for *Trpc1*, *Pgc-1α*, *Myog* as well as *Igf1*[48] were shown to increase in the leg musculature of PEMF-treated mice (Figure 1C), corroborating NFAT/calcineurin-mediated oxidative muscle enhancement in vivo,[23,26-29] and demonstrating genetic and developmental

TABLE 2 Myogenic gene modulation by weekly PEMF intervention. Gene expression following 6 weeks of PEMF/exercise intervention in the Soleus and EDL

	Skeletal muscle							
		Sedentary		Exercise				
		0 mT	1.5 mT	0 mT	1.5 mT			
		Group 1	Group 2	Group 3	Group 4			
		–E/–P	–E/+P	+E/–P	+E/+P	Two-way ANOVA *P* values		
	Genes	Mean (SD)				PEMF vs no PEMF	Exercise vs no exercise	PEMF & exercise interaction
Soleus	*Pgc-1α*	0.72 (0.32)	1.00 (0.44)	0.74 (0.67)	1.56 (0.74)	**0.03**	0.25	0.28
					***P* = .03 wrt 1**			
					***P* = .02 wrt 3**			
	Cpt1b	0.77 (0.57)	1.73 (1.22)	1.4 (0.92)	2.36 (2.00)	0.10	0.27	1.00
	Nampt	0.90 (0.53)	1.39 (0.78)	1.07 (0.6)	2.01 (1.75)	0.12	0.38	0.62
	Sirt1	0.60 (0.25)	2.08 (1.17)	2.20 (1.84)	2.37 (1.85)	0.22	0.17	0.33
	Vegf-a	0.84 (0.30)	1.91 (1.00)	1.58 (1.29)	1.35 (1.09)	0.34	0.84	0.14
	Mef2c	0.83 (0.59)	1.78 (0.81)	1.28 (0.95)	1.7 (1.19)	0.11	0.65	0.52
	Fndc5	0.74 (0.39)	1.37 (0.93)	1.51 (0.86)	1.55 (0.93)	0.35	0.19	0.40
	Trim55	0.8 (0.61)	1.61 (2.0)	1.81 (1.33)	2.52 (2.63)	0.34	0.23	0.95
	Gasp1	0.88 (0.32)	2.34 (2.03)	1.40 (0.90)	1.09 (1.30)	0.31	0.52	0.13
EDL	*Pgc-1α*	1.02 (0.69)	3.35 (3.58)	1.78 (1.12)	1.90 (2.66)	0.29	0.76	0.34
	Cpt1b	0.93 (0.61)	3.59 (4.18)	1.54 (1.31)	1.84 (2.46)	0.25	0.65	0.35
	Nampt	0.99 (0.51)	2.47 (1.93)	1.90 (1.46)	1.70 (1.91)	0.40	0.93	0.27
	Sirt1	1.01 (0.92)	2.30 (2.74)	1.18 (1.17)	1.54 (1.90)	0.36	0.74	0.60
	Vegf-a	0.96 (0.44)	0.94 (0.48)	0.73 (0.32)	1.03 (0.57)	0.51	0.76	0.47
	Mef2c	0.83 (0.42)	2.94 (5.06)	1.24 (0.70)	2.01 (2.06)	0.31	0.85	0.63
	Trim55	1.75 (1.98)	1.43 (1.54)	0.54 (0.22)	1.07 (1.36)	0.87	0.22	0.51
	Gasp1	1.08 (0.48)	3.55 (3.80)	1.28 (1.10)	1.68 (0.88)	0.18	0.42	0.32

Note: The left side of the table shows the mean and standard deviation of gene expression levels in each group. The right side of the table shows the *P* values from two-way analysis of variance analyses to test the effects of PEMF and exercise, and the statistical interaction between the two. The *P* values in bold indicate the *P* values from the test of differential expression between one group in the column with regards to (wrt) another group, using Tukey's test for multiple pairwise comparisons.

symmetry with previous in vitro findings.[36] Myogenin cooperates with NFAT and TRPC1 to enhance oxidative muscle capacity[47,49] and positively correlates with mitochondrial respiratory capacity in oxidative fibers.[45] IGF-1 is a myokine promoting muscle regeneration, whose expression is greatest in highly oxidative fibers.[44] The transcript levels of *Cd36* (mitochondrial fatty acid translocase; FAT) were also increased with PEMF treatment (Figure 1C), aligning with previously described PGC-1α-stimulated mitochondrial fatty acid uptake and mitochondriogenesis,[50] enhancing systemic fatty acid oxidation and insulin-sensitivity.[51] Accordingly, the resting respiratory exchange ratio (RER), a described metabolic adaptation to PGC-1α upregulation,[52] commenced to drop 5 weeks after commencement of PEMF treatment, corroborating PGC-1α-dependent enhancement of fatty acid oxidation as a result of our magnetic paradigm (Figure 1D). Serum insulin levels were also reduced by PEMF treatment (Figure 1E), paralleling accepted exercise-induced adaptations including enhanced oxidative muscle expression, fatty acid oxidation, and insulin-sensitivity.[51,53] Weekly PEMF treatment (10 min/week) for a few months hence recapitulates key aspects of the systemic benefits typically associated with exercise.[51]

3.2 | Short-term weekly PEMF treatment potentiates the effects of exercise

Endurance exercise increased muscular PGC-1α expression[51] to a comparable degree as weekly PEMFtreatment

(Figure 1C), suggesting a correlation between exercise and PEMF exposure. Given that systemic fatty acid oxidation commenced to increase (reduced RER) 5 weeks after commencing PEMF treatment (Figure 1D), we examined the combined effects of short-term PEMF treatment, alone or combined with exhaustive exercise. Mice were ran to exhaustion thrice weekly in conjunction with weekly PEMF exposure (1.5 mT for 10 minutes). After 5 weeks of exhaustive running, mice undergoing PEMF treatment (blue) commenced to out-perform control counterparts (red; Figure 2A); that moreover, commenced to show signs of overtraining at 5 weeks. Notably, strenuous exercise raised leptin (Figure 2B) and insulin (Figure 2C) levels that were normalized with concomitant PEMF treatment. These results agree with data demonstrating stress induces elevations in serum leptin levels,[54] a response that appeared to be ameliorated in response to PEMF treatment.

The Soleus and EDL represent muscles of the leg characterized by high and low oxidative capacities, respectively.[25] Two-way ANOVA statistical analyses detected significant

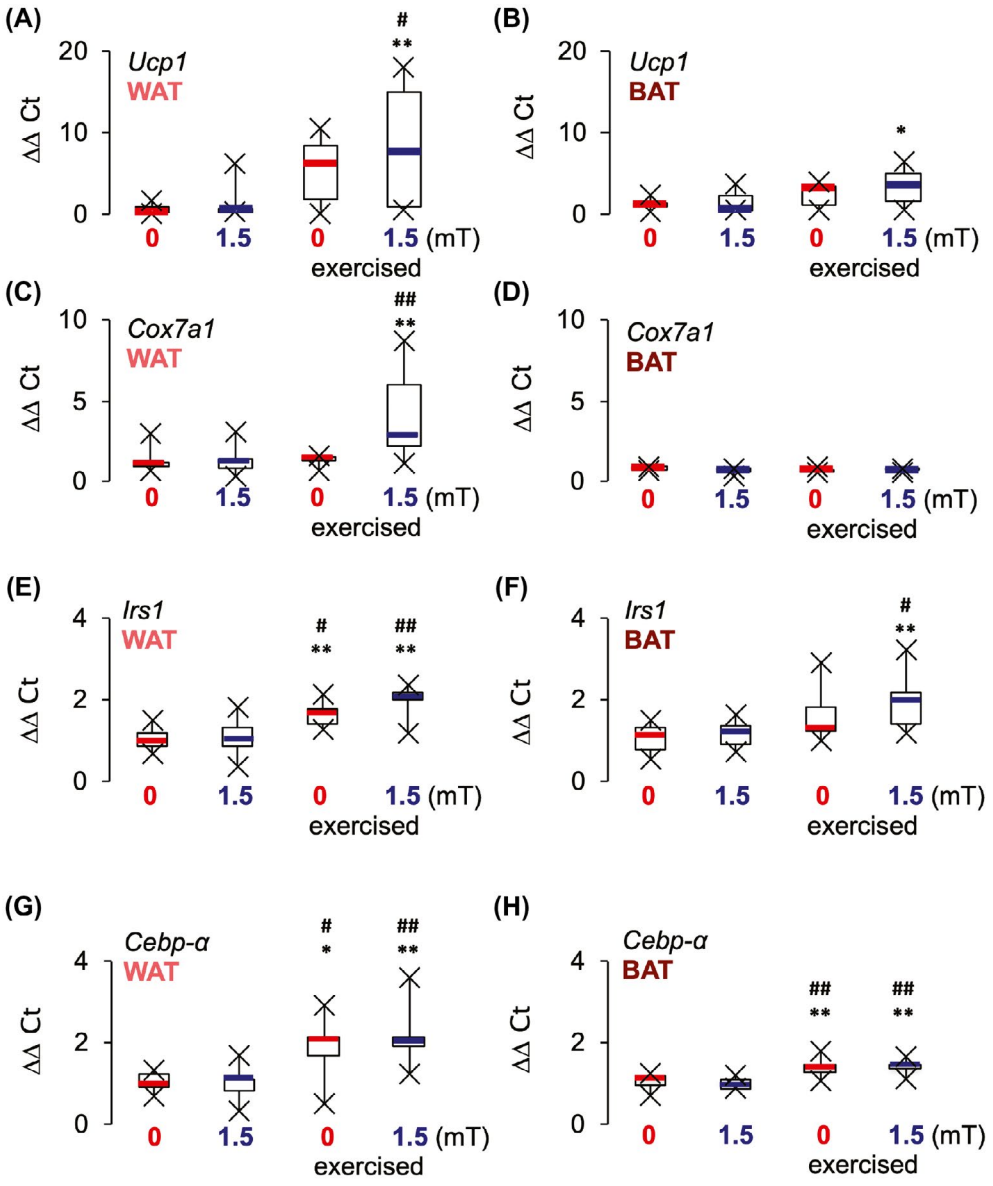

FIGURE 3 PEMF treatment accentuates adipose browning and insulin-sensitivity in response to exercise. *Ucp1* transcript levels increased in inguinal white adipose tissue (A; WAT), but not interscapular brown adipose tissue (B; BAT), following 6 weeks PEMF intervention (10 min/week) in conjunction with exhaustive exercise. *Cox7a1* transcript levels increased in WAT (C), but not BAT (D), following weekly PEMF intervention and exhaustive exercise interventions. *Irs1* transcript levels increased in both WAT (E) and BAT (F) following weekly PEMF intervention and exhaustive exercise interventions, but only in WAT by exercise alone (E). *Cebp-α* gene expression was increased in WAT (G) and BAT (H) by exercise with and without PEMF treatment. All means are derived from six female mice/condition. ** and *$P < .01$ and $< .05$, respectively, wrt correspondent 0 mT (non-exercised) and ## and # $P < .01$ and $< .05$, respectively, wrt correspondent 1.5 mT (non-exercised) by two-way ANOVA. See Table 3 for further details. Mice were exposed to PEMFs for 10 min/week for 6 weeks.

increases in *Pgc-1α* gene expressions in Solei of the PEMF plus exercise (+E/+P) cohort, compared to the unexercised (–E/–P) or exercised (+E/–P) cohorts, but not from PEMF-treated mice (–E/+P), reflecting a significant interaction with PEMF treatment (Table 2). On the contrary, significant changes in gene expression in the EDL were not achieved in any of the cohorts. Statistically significant elevations in *Pgc-1α* expression preceded that of the other Solei genes at 6 weeks. Paired *t* tests of the distinct intervention cohorts against the control cohorts (–E/–P) corroborated increases in *Pgc-1α* in the dual intervention cohort of mice (+E/+P) for Solei (Figures 2D, S3A), but not EDL (Figures 2E, S3B), as well as revealed a general trend for genes associated with PGC-1α (*Sirt1*, *Mef2c*), oxidative muscle expression (*Vegf-a, Nampt, Trim55*, *Gasp1*), or fat metabolism (*Cpt1β*, *Fndc5*) (Supplemental Figure S3), whereby PEMF treatment alone (–E/+P) raised gene expression in the Soleus over control levels (–E/–P), often approaching or surpassing that of the exercise alone (+E/–P) or exercise plus PEMF treatment (+E/+P) groups. Notably, statistical significance was observed for the Solei genes, *Sirt1*, *Mef2c*, and *Vegf-a*, in the PEMF-treated alone (–E/+P) cohort relative to controls (–E/–P), whereas exercised mice, with (+E/+P) or without (+E/–P) PEMF treatment, were not statistically different from sham controls (–E/–P). MEF2C promotes PGC-1α expression[23,46,55-57] and correlates with NFATC1 expression pattern[36,58] that precedes and predicts oxidative muscle development.[59] SIRT1 stimulates PGC-1α expression, upstream of mitochondriogenesis and metabolic balance.[11] VEGFA is an angiogenic myokine upregulated by PGC-1α and exercise.[60,61] *Mef2c*, *Sirt1*, and *Vegf-a* were all upregulated by PEMF treatment alone (–E/+P) in Solei (Figures 2F, S3C,E, respectively), but not EDL (Figures 2G, S3D,F, respectively). Therefore, 60 minutes of total PEMF exposure (distributed over 6 weeks) was sufficient to upregulate the expression of mitochondrial genes associated with PGC-1α (*Mef2c* and *Sirt1*), whereas genes related to muscle hypertrophy (*Gasp1* and *Trim55*) or metabolic adaptations (*Nampt*, *Cpt1β*, and *Fndc5*) exhibited only nonsignificant elevations at 6 weeks in response to PEMF exposure, with or without exhaustive exercise.

3.3 | Adipogenic consequences of short-term weekly PEMF treatment and exercise

The adipogenic consequences of short-term PEMF treatment in combination with exercise (+E/+P) were relatively strong compared to those of skeletal muscle. Nonetheless, direct PEMF exposure had little effect over thermogenic gene expression in isolated adipocytes derived from either WAT or BAT deposits (Supplemental Figure S4), suggesting that the in vivo adipose tissue-specific effects arose from muscle, presumably via the secretion of myokines,[31-33,62,63] such as IGF-1 (Figure 1C) and VEGFA (Figure S3E), and aligning with the fact that the observed changes were induced by exercise that directly recruits the activity of muscle.

Adipose samples from the combined PEMF-treated and exercised cohort (+E/+P) showed greater elevations of *Ucp1* and *Cox7a1* in WAT (subcutaneous inguinal) (Figure 3A,C), respectively, than in BAT (interscapular) (Figure 3B,D; Table 3), respectively, reflecting the involvement of these genes in white adipose browning, mitochondriogenesis and lipid oxidation,[64] and paralleling previously demonstrated disparate exercise-induced thermogenic responses of the inguinal (WAT) vs interscapular (BAT) adipose deposits.[65] *Pgc-1α* expression was significantly elevated in both WAT and BAT by the combination of exercise and PEMF treatment (+E/+P) relative to sham control (–E/–P) and exercised alone (+E/–P) groups, but not from the PEMF alone cohort (–E/+P) (Table 3), recapitulating the same *Pgc-1α*-PEMF interaction detected in the Soleus muscle (Table 2; Figures 3D, S3A). The expression levels of the insulin receptor substrate 1 (*Irs1*) gene, mediator of insulin, and IGF signaling pathways,[66] was upregulated in WAT by exercise alone (+E/–P) (Figure 3E) and in WAT and BAT by combined exercise and PEMF treatment (+E/+P) (Figure 3E,F, respectively), corroborating that beiged WAT (Figure 3A,C) induced by PEMF exposure, exhibits greater insulin-sensitivity.[67] *Cebp-α* expression was elevated by both exercise alone (+E/–P) and in combination with PEMF treatment (+E/+P) in both WAT (Figure 3G) and BAT (Figure 3H), reflecting its reported positive association with insulin-sensitivity and negative relationship to adipose mass.[68] *Glut4* (*Slc2a4*) gene expression was elevated by exercise alone (+E/–P) in both WAT and BAT and further augmented by supplemental PEMF treatment (+E/+P) only in WAT (Table 3), paralleling findings that exercise either enhances or suppresses glucose uptake in WAT and BAT, respectively.[69] Provocatively, the inhibition of insulin-mediated glucose uptake into BAT by exercise has been previously shown to be inversely correlated with inflammatory status.[69] Notably, our exhaustive exercise paradigm (+E/–P) raised leptin (*Lep*) transcript levels in WAT and BAT that were normalized in WAT with the addition of PEMF treatment (+E/+P) (Table 3), as previously shown serologically from these same mice (Figure 2B). Finally, nicotinamide phosphoribosyltransferase (*Nampt*) gene expression was enhanced in BAT, but not WAT, by the combination of exercise and PEMF treatment (+E/+P) (Table 3), underlying its positive correlation to insulin-sensitivity, adiponectin levels, fatty acid oxidation, and PPAR signaling.[70] Therefore, short-term (6 weeks) weekly (10 min/week) PEMF treatment of mice was sufficient to accentuate the onset of known physical (Figure 2) and metabolic (Figures 1-3) adaptations commonly associated with exercise that previously have been positively correlated with PGC-1α expression.

TABLE 3 Systemic adipogenic modulation by weekly PEMF intervention. Gene expression following 6 weeks of PEMF/exercise intervention in brown (interscapular) and white (subcutaneous inguinal) adipose samples

	Sedentary		Exercise				
	0 mT	1.5 mT	0 mT	1.5 mT			
	Group 1	Group 2	Group 3	Group 4			
	–E/–P	–E/+P	+E/–P	+E/+P	Two-way ANOVA *P* values		
Genes	Mean (SD)				PEMF vs no PEMF	Exercise vs no exercise	PEMF & exercise interaction
White adipose tissue							
Pgc-1α	0.56 (0.24)	0.80 (0.25)	0.53 (0.18)	1.06 (0.35) ***P* = .004 wrt 1** ***P* = .002 wrt 3**	**0.002**	0.30	0.18
Ucp1	0.51 (0.60)	1.51 (2.62)	5.3 (4.28)	8.32 (8.02) ***P* = .01 wrt 1** ***P* = .03 wrt 2**	0.32	**0.01**	0.61
Cox7a1	1.35 (0.86)	1.37 (0.93)	1.33 (0.33)	4.09 (3.01) ***P* = .01 wrt 1** ***P* = .01 wrt 2** ***P* = .01 wrt 3**	**0.05**	0.06	0.05
Glut4	1.07 (0.46)	1.27 (0.69)	2.14 (1.03) ***P* = .02 wrt 1** ***P* = .05 wrt 2**	2.64 (0.53) ***P* = .001 wrt 1** ***P* = .003 wrt 2**	0.23	**<0.001**	0.61
Irs1	1.03 (0.29)	1.09 (0.5)	1.65 (0.32) ***P* = .01 wrt 1** ***P* = .02 wrt2**	1.98 (0.41) ***P* < .001 wrt 1** ***P* = .001 wrt 2**	0.23	**<0.001**	0.40
Lep	0.65 (0.27)	0.48 (0.28)	1.20 (0.62) ***P* = .03 wrt 1** ***P* = .01 wrt 2**	0.88 (0.41)	0.18	**0.01**	0.66
Nampt	1.05 (0.22)	0.99 (0.51)	0.98 (0.4)	1.55 (0.34)	0.15	0.16	0.08
Cebp-α	1.03 (0.26)	1.01 (0.46)	1.88 (0.80) ***P* = .03 wrt 1** ***P* = .03 wrt 2**	2.17 (0.79) ***P* = .005 wrt 1** ***P* = .004 wrt 2**	0.60	**0.001**	0.56
Fasn	1.83 (1.6)	4.60 (3.58)	2.20 (1.51)	4.21 (2.55)	**0.03**	0.99	0.72
AdipoQ	1.01 (0.11)	1.09 (0.40)	0.98 (0.41)	1.08 (0.53)	0.56	0.92	0.96
Prdm16	0.70 (0.22)	1.09 (0.58)	0.83 (0.40)	1.01 (0.36)	0.10	0.88	0.54
Elovl3	6.04 (7.83)	10.37 (10.51)	2.71 (1.72)	7.71 (5.98)	0.13	0.32	0.91
Dio2	1.72 (1.53)	2.63 (2.00)	1.38 (0.32)	3.00 (2.64)	0.13	0.99	0.67
Brown adipose tissue							
Pgc-1α	1.14 (0.62)	1.88 (0.99)	1.06 (0.61)	2.58 (1.80) ***P* = .04 wrt 1** ***P* = .03 wrt 3**	**0.02**	0.50	0.40
Ucp1	1.15 (0.71)	1.37 (1.4)	2.37 (1.52)	3.35 (2.44) ***P* = .03 wrt 1**	0.39	**0.03**	0.58
Cox7a1	0.84 (0.14)	0.67 (0.20)	0.74 (0.13)	0.74 (0.08)	0.18	0.78	0.17

(Continues)

TABLE 3 (Continued)

	Sedentary		Exercise				
	0 mT	1.5 mT	0 mT	1.5 mT			
	Group 1	Group 2	Group 3	Group 4			
	–E/–P	–E/+P	+E/–P	+E/+P	Two-way ANOVA *P* values		
Genes	Mean (SD)				PEMF vs no PEMF	Exercise vs no exercise	PEMF & exercise interaction
Glut4	1.08 (0.42)	1.06 (0.33)	1.99 (0.86) ***P* = .01 wrt 1** ***P* = .01 wrt 2**	1.65 (0.46)	0.433	**0.003**	0.487
Irs1	1.06 (0.37)	1.18 (0.34)	1.62 (0.72)	1.99 (0.75) ***P* = .01 wrt 1** ***P* = .02 wrt 2**	0.31	**0.009**	0.60
Lep	1.17 (0.67)	1.02 (0.79)	2.02 (0.76) ***P* = .041 wrt 1** ***P* = .019 wrt 2**	0.73 (0.41) ***P* = .004 wrt 3**	**0.02**	0.32	0.05
Nampt	6.65 (1.06)	4.83 (1.49)	6.96 (2.38)	9.02 (3.86) ***P* = .01 wrt 2**	0.91	**0.04**	0.07
Cebp-α	1.02 (0.21)	0.96 (0.14)	1.37 (0.24) ***P* = .006 wrt 1** ***P* = .002 wrt 2**	1.38 (0.18) ***P* = .005 wrt 1** ***P* = .002 wrt 2**	0.7809	**<0.001**	0.6781
Fasn	0.80 (0.31)	0.89 (0.23)	0.77 (0.31)	0.77 (0.40)	0.73	0.55	0.75
AdipoQ	1.04 (0.17)	1.08 (0.25)	0.98 (0.23)	1.11 (0.26)	0.37	0.89	0.59
Prdm16	0.81 (0.26)	0.77 (0.42)	0.70 (0.32)	0.98 (0.22)	0.37	0.71	0.22
Elovl3	1.03 (0.38)	1.40 (0.64)	1.22 (0.58)	1.37 (0.62)	0.27	0.73	0.63
Dio2	1.27 (0.72)	1.52 (1.26)	1.40 (1.04)	3.53 (2.86)	0.10	0.14	0.19

Note: The left side of the table shows the mean and standard deviation of gene expression levels in each group. The right side of the table shows the *P* values from two-way analysis of variance analyses to test the effects of PEMF and exercise, and the statistical interaction between the two. The *P* values in bold indicate the *P* values from the test of differential expression between one group in the column with regards to (wrt) another group, using Tukey's test for multiple pairwise comparisons.

3.4 | Systemic mitohormetic responses to PEMF treatment

Given that mice commenced to show signs of duress after 6 weeks of thrice weekly exhaustive exercise (Figure 1), another study was undertaken to examine the combined effects of PEMF exposure and more moderate exercise, twice weekly, conducted for 8 weeks. By contrast with 6 weeks of treatment where PEMF exposure alone (–E/+P) produced significant upregulations in only a subset of genes, 8 weeks of exposure was sufficient to detect significant changes in the expression for all candidate genes involved in systemic mitohormetic adaptations (Figure 4; *cf* Figure S3). PGC-1α is a master regulator of mitochondriogenesis, subject to regulation by SIRT1,[11] and is responsible for initiating skeletal muscle mitohormetic adaptations to endurance exercise.[71] PGC-1α-mediated mitohormetic adaptations occur through interactions with other transcription factors including myocyte enhancer factor-2 (MEF2C), peroxisome proliferator-activated receptor-α (PPAR-α), and nuclear respiratory factors 1 and 2 (NRF1/2).[57] Mitochondrial transcription factor A (TFAM) regulates mitochondriogenesis resulting from this same transcriptional cascade,[57,72] downstream of superoxide dismutase 2 (SOD2) upregulation, also strongly implicated in systemic mitohormesis.[72,73] Transcription factor EB (TFEB) regulates exercise-mediated muscle mitochondriogenesis and establishes metabolic flexibility,[15] including enhanced fatty acid oxidation (Figure 1D), in coordination with PGC-1α activation.[74] Finally, NAD(P)H dehydrogenase [quinone] 1 gene (NQO1) is a participant of the PGC-1α-NRF2 transcriptional cascade that governs mitohormetic adaptation against oxidative stress.[73,75,76] Significant upregulations in the expression of these genes were consistently observed in response to PEMF treatment alone (–E/+P), and less often with exercise alone (+E/–P) or combination treatment (+E/+P) (Figure 4A-J). The sum of these data indicate that PEMFs instill PGC-1α-associated mitohormetic adaptations in vivo, paralleling our previous in vitro findings.[36]

PGC-1α activation has been shown to stimulate free fatty acid oxidation and myokine production,[77] associated with mitochondrial upregulation.[31,78] Insulin levels incrementally decreased between treatment groups, ultimately reaching significance for the dual PEMF-treated and exercised cohort (+E/+P) at 8 weeks (Figure 4K). Accordingly, adiponectin, a myokine/adipokine with insulin-sensitizing attributes,[79] rose incrementally between ascending groups until reaching significance in the dual intervention cohort (+E/+P) (Figure 4L). Adiponectin levels have been shown to positively correlate with adipose PGC-1α and UCP1 levels,[24] giving a greater context to these adiponectin results and adipose transcript analyses per condition (Figure 3 and Table 3). The levels of interleukin-6 (IL-6), the prototypical myokine,[62,63] showed a tendency to rise in response to 8 weeks of PEMF treatment alone (–E/+P), but failed to reach statistical significance (Figure 4M). Serum leptin (adipokine) levels are known to be lowered by exercise training (≥ 2 weeks) and positively correlate with obesity and systemic inflammation.[80] Leptin levels were found to drop in mice treated with PEMFs alone (–E/+P) (Figure 4N). VEGFA is a pro-angiogenic myokine upregulated by PGC-1α in response to exercise[60,61] and notably, was the only gene, not directly related to mitochondriogenesis, upregulated at 6 weeks in response to PEMF exposure alone (Figure S3E). IGF-1 is another myokine[62] whose expression was shown to be upregulated by PEMF exposure (Figure 1C) and is known to be highly expressed in oxidative muscle.[44] Myokine production and release may hence be one limb of a greater systemic mitohormetic response that is capable of being evoked by PEMF treatment.

3.5 | Diversity and composition of gut microbiota

The cecal and fecal microbiomes from our distinct mouse cohorts were similar in composition and did not show a large degree of variation at the OTU level. Therefore, rather than comparing gut segment-dependent changes, we pooled cecal and fecal microbiomes and analyzed them as a unit. The richness and diversity of the gut microbiota (fecal and cecal microbiomes) of mice subjected to the four treatment groups were estimated using the Chao1 and Simpson's indices, respectively (Figure 5A). Based on the Simpson index, the microbiomes of the sedentary cohort (–E/–P) exhibited the greatest level of diversity. At the level of phyla their microbiomes were dominated by OTUs affiliated to *Bacteroidetes* (48%-57%), *Firmicutes* (36%-43%), *Deferribacteres* (3%-5%) and *Proteobacteria* (1%-2%) (Figure 5B, Table S1). An increase in the ratio of *Firmicutes*/*Bacteroidetes* (F/B) has been shown to correlate with obesity in humans and mice and is associated with a greater capacity for energy harvest from the diet.[81] The F/B ratio was highest in the sedentary (–E/P) group (1.0), followed by the PEMF-alone group (–E/+P; 0.8), then, the exercised alone (+E/–P; 0.6) and combination intervention (+E/+P; 0.6) groups (Figure 5C), suggestive of a leaner phenotype in mice receiving PEMF treatment, with or without exercise. A state of leanness in exercised and PEMF-treated mice (+E/+P) would be metabolically complemented by the observed enhancements in adipose browning (Figure 3, Table 3), oxidative muscle development (Table 2 and Figures 1, S3), and PGC-1α upregulations in muscle and adipose tissues (Figures 1, 2, S3, and Tables 2, 3).

A PCO analysis of transformed OTU data sets from fecal and cecal microbiome samples showed distinct compositional differences in the gut microbiota between the four treatment groups that was statistically verified by a PERMANOVA test ($P = .001$ in 999 permutations) (Figure 5D). A PICRUSt analyses was next run to determine the functional roles of the gut microbiomes of mice from the distinct treatment groups using 16S rRNA gene profiling. Pearson correlations ($R > 0.6$) were used to identify taxon-specific functions exhibiting linear correlations to gut microbiome communities and linked to particular KEGG (Kyoto Encyclopedia of Genes and Genomes) pathways (grey circle; also see Supplemental Figure S6).

3.6 | Effect of PEMF treatment on the gut microbiomes of sedentary and exercised mice

LEfSe analysis was used to compare microbiome responses of the different treatment groups. Unexercised control mice (–E/–P) showed greater abundances of bacterial OTUs pertaining to *Bacteroidetes* (3 OTUs), *Firmicutes* (10 OTUs), *Tenericutes* (4 OTUs), and *Proteobacteria* (2 OTUs) (Figure 6A; red). By contrast, unexercised, but PEMF-treated mice (–E/+P), showed greater abundances of OTUs belonging to the phyla *Tenericutes* (6 OTUs) and *Acinetobacteria* (5 OTUs) (Figure 6A; blue). At a deeper taxonomic level, the unexercised control mice (–E/–P) exhibited greater compositional diversity in OTUs pertaining to *Rikenellaceae spp., Bacilli spp., Turicibacteriales spp., Clostridiaceae spp., Anaeroplasmatales spp.,* and *Bilophila spp*., whereas for the unexercised, but PEMF-treated mice (–E/+P), the OTUs assigned to *Tenericutes* and *Acinetobacteria* showed lineages associated with *Mollicutes*/RF39 and *Coriobacteriales spp., Adlercreutzia spp*., respectively. Therefore, weekly PEMF exposure per se was capable of producing changes in the gut microbiota.

Exercise also elaborated unique differences in gut microbiomes that further individualized with supplemental PEMF treatment (Figure 6B). The combination of exercise and PEMF treatment (+E/+P; blue) elaborated greater abundances of OTUs assigned to *Bacteroidetes* (8 OTUs), *Firmicutes* (2 OTUs), *Proteobacteria* (4 OTUs), whereas exercise alone (+E/–P; red) produced elevations in *Bacteroidetes* (3 OTUs), *Verrucomicrobia* (6 OTUs), *Firmicutes* (2 OTUs), and *Acinetobacteria* (2 OTUs). Specifically, the combination of

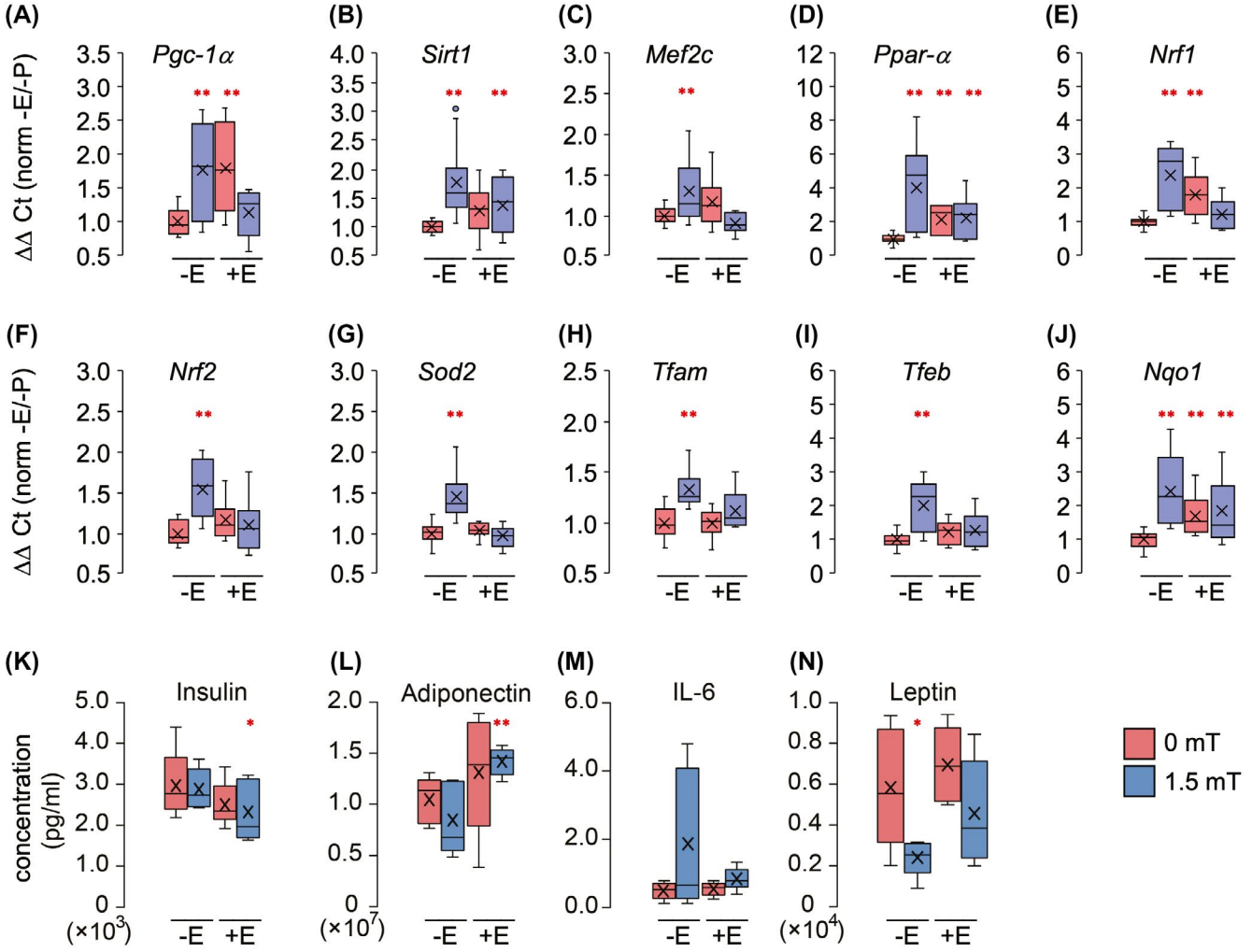

FIGURE 4 Mitohormetic genetic responses to PEMF exposure in the absence or presence of moderate exercise. A-J, Relative expression for the indicated mitohormetic genes. All values were normalized to control scenarios (–E/–P) shown in red far left. K-L, Absolute serum levels for the indicated blood markers. Mice were exposed to 1.5 mT PEMFs for 10 min/week for 8 weeks with and without moderate exercise consisting of twice per week running to exhaustion. All data were generated from a pool of five mice per condition. For each histogram the 1st, 2nd, 3rd, and 4th bars correspond to our previously delineated (–E/–P), (–E/+P), (+E/–P), and (+E/+P) cohort interventions, respectively. Red and blue bars correspond to 0 mT and 1.5 mT PEMF exposures in the absence (–E) or presence (+E) of twice weekly running exercise as indicated. ** and *$P < .01$ and $< .05$, respectively, wrt unexercised control (–E/+P).

exercise and PEMF treatment (+E/+P) produced enrichments in *Bacteroidales spp., Prevotella spp*., *Ruminococcus spp*., *Proteus spp*., *Betaproteobacteria spp*., and *Burkholderiales spp*., whereas exercise alone (+E/–P) enriched for *Bacteroidales spp., Verrucomicrobiales spp., Akkermansia muciniphila, Coprobacillus spp.,* and *Coriobacteriaceae spp*.

4 | DISCUSSION

4.1 | PGC-1α mediates systemic effects of PEMF treatment

Brief PEMF exposure has been shown to stimulate TRPC1-NFAT-dependent transcriptional cascades, driving PGC-1α-dependent in vitro mitochondriogenesis and myogenesis, while exhibiting a genetic propensity toward the oxidative phenotype.[36] Here, we show that analogous PEMF exposure of mice (10 min/week) similarly accentuated NFAT-regulated gene expression for *Pgc-1α*, *Trpc1*, *Igf-1*, and *Myog* (Figure 1), while enhancing oxidative muscle expression (Figure 1) and improving physical capacity (Figure 2). Thus, the upregulation of PGC-1α-dependent mitochondrial and oxidative pathways was common to both the in vitro[36] and in vivo PEMF-treated scenarios. PGC-1α is necessary for the establishment of systemic mitohormetic adaptations[73] involving oxidative muscle.[23,71,75,82] As a result of enhanced PGC-1α deployment oxidative muscle exhibits a heightened propensity for fatty acid oxidation and insulin-sensitivity.[24,51,52] Accordingly,

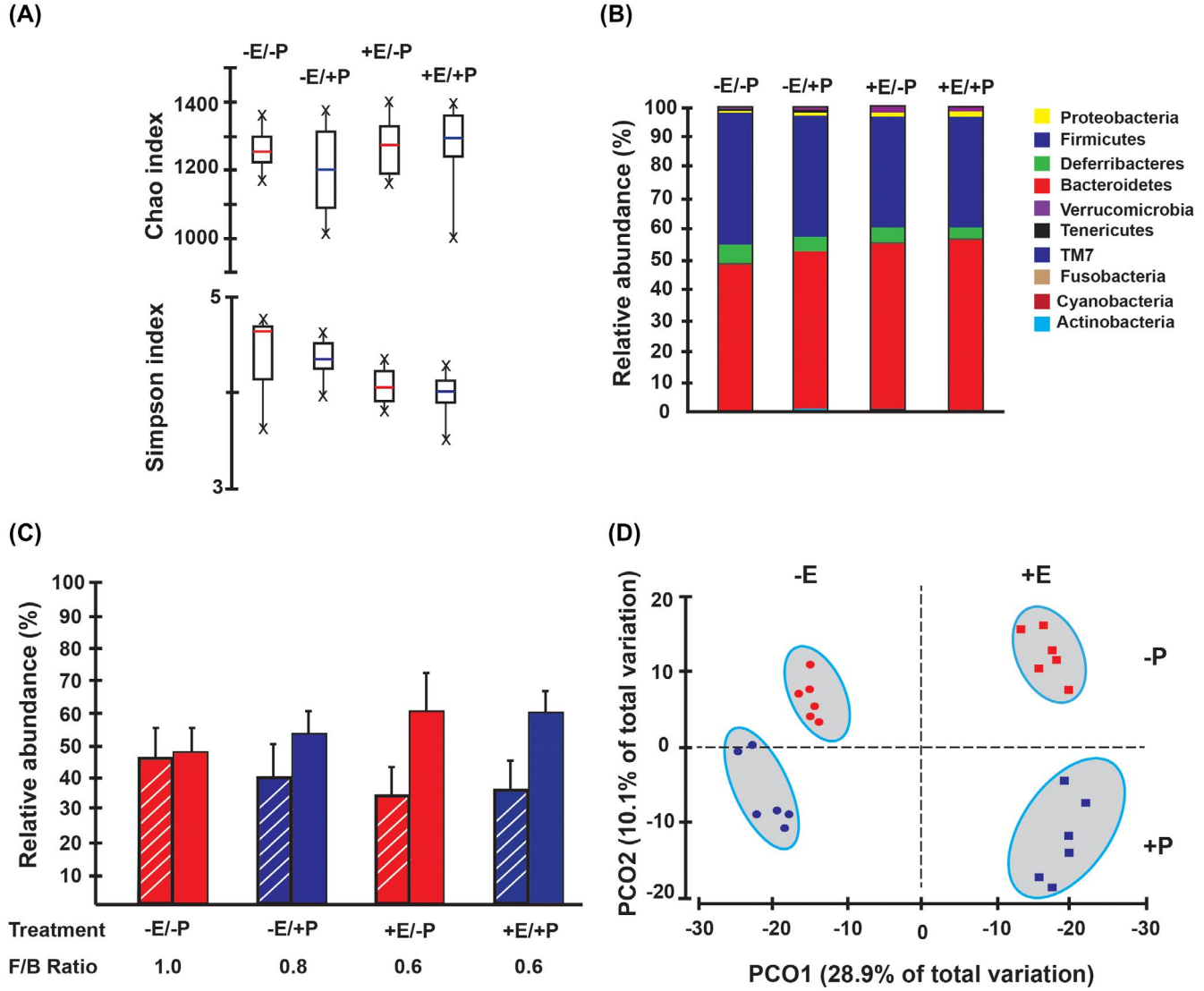

FIGURE 5 Diversity and characteristics of gut microbial community in female mice of different intervention groups. A, Alpha diversities (Chao1 and Simpson indices) of microbial communities in fecal and cecal contents of mice. B, Relative abundance of OTUs (assigned to the Phyla level) in the gut microbiomes of mice. C, Relative abundance and ratios of OTUs assigned to *Firmicutes* (hatched) and *Bacteroidetes* (solid). D, A Principal Coordinate Analysis (PCO) of microbial communities in fecal and cecal contents of mice from the four treatment groups. The microbiomes of different treatment groups are indicated by color and a PERMANOVA (Permutational multivariate analysis of variance) test indicate significant differences ($P = .001$) in OTU composition between treatments. Pairwise PERMANOVA tests between each treatment showed significant differences ($P < .05$).

PGC-1α suppression characterizes diabetes-related muscle atrophy.[56] Here, we detected PEMF-induced upregulation of muscular *Cd36*, a mitochondrial fatty acid translocase (Figure 1C), enhanced systemic fatty acid oxidation (Figure 1D) and reduced serum insulin levels (Figure 1E), emulating the metabolic effects more commonly associated with exercise.[51-53] Notably, combining PEMF exposure with exercise accelerated the onset of *Pgc-1α* expression (Figure 2). PEMF treatment is thus capable of recapitulating recognized metabolic adaptations associated with endurance exercise that were dependent on PGC-1α-induced muscular mitochondriogenesis.[44,72]

Changes in the microbiome composition and function are also accepted exercise adaptations.[2,83,84] We observed unique shifts in gut microbiome composition, paralleling changes in metabolic capacities, following PEMF treatment alone or in combination with exercise. Combining PEMF treatment with short-term exercise enhanced *Pgc-1α* expression in skeletal muscle, WAT and BAT, whereas exercise alone did not (Figure 2D). On the contrary, longer-term endurance exercise[72] or PEMF exposure (Figure 1C) are either capable of upregulating *Pgc-1α* expression and downstream mitochondriogenesis. The fact that the PPAR/PGC-1α mitochondrial pathways and the microbiome interact for mutual

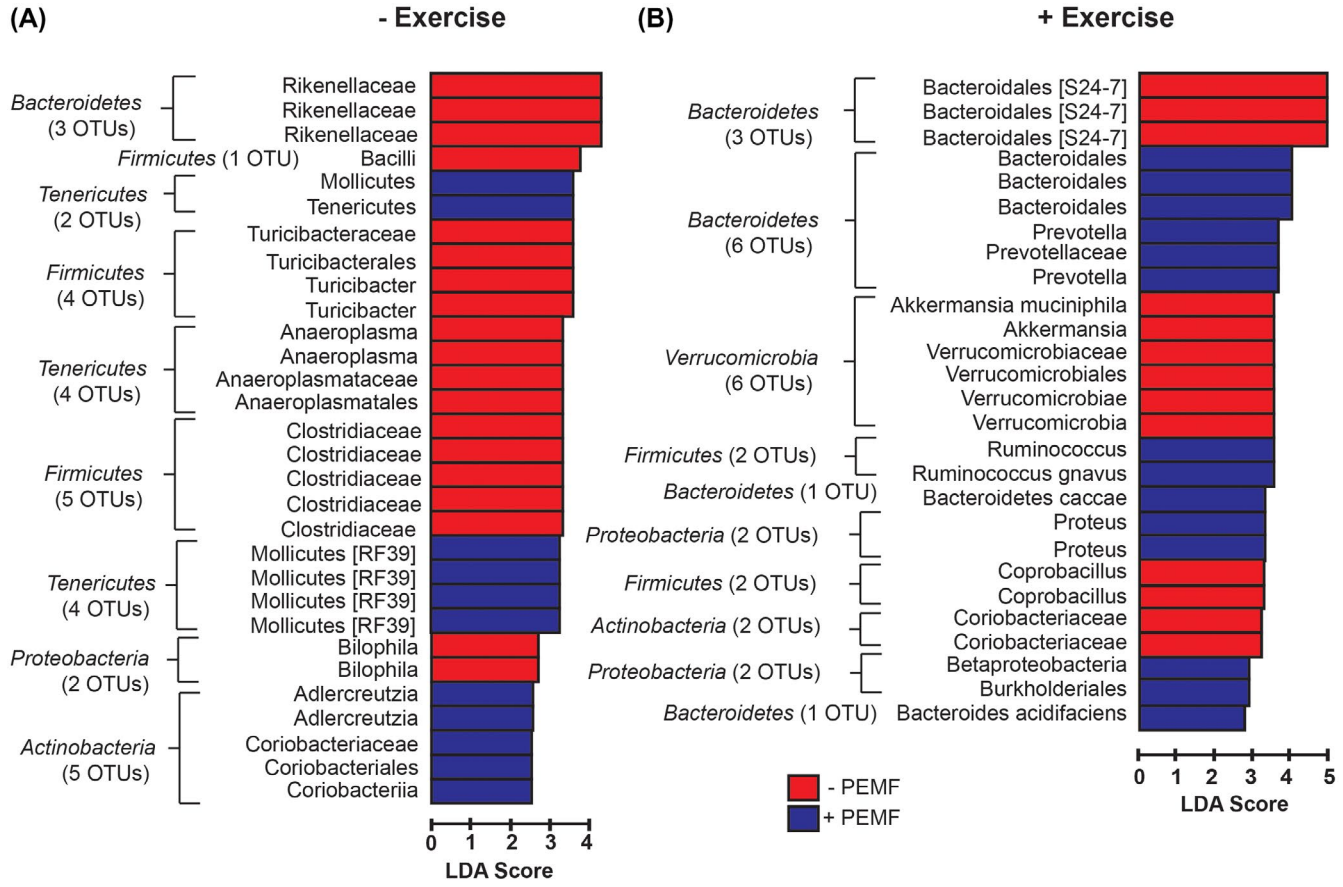

FIGURE 6 Taxonomic differences between the gut microbiomes of (A) unexercised, PEMF-treated (–E/+P; blue) and non-PEMF-treated (–E/−P; red) and (B) exercised, PEMF-treated (+E/+P; blue) and non-PEMF-treated (+E/−P; red) cohorts of female mice by linear discriminant analysis effect size (LEfSe) analysis. Cladograms represented by the LDA model show differentially abundant OTUs for paired treatment groups being tested.

reinforcement in effect closes the loop between muscle (large activatable pool of mitochondria) and microbiome function.[85] Indeed, bidirectional communication between the gut microbiome and muscle mitochondria is now supported by numerous studies demonstrating that muscle mitochondria and the commensal gut microbiota cross talk (via the SCFAs that potentiate PGC-1α function) to modulate redox balance and systemic inflammation.[17,86,87]

Adipose beiging is another accepted exercise adaptation that is likewise dependent on PGC-1α expression and associated changes in mitochondrial function and biogenesis.[88,89] In the short-term, the combination of PEMF treatment plus exercise (+E/+P) upregulated *Pgc-1α* and *Ucp1* expression in WAT and BAT (Table 3) as well as produced alterations in gut microbiome composition indicative of reduced adiposity (Figure 5). Obesity is associated with a high F/B ratio in mice[90] and humans.[91] Our unexercised control group of mice (–E/–P) exhibited the highest F/B ratio (1.0) with PEMF treatment alone (–E/+P) contributing a reduction in the ratio to 0.8; exercise alone (+E/–P) or the combination of PEMF treatment and exercise (+E/+P) lowered the F/B ratio further to a common level of 0.6 (Figure 5). PEMF treatment hence induced similar, albeit more modest, shifts in the gut microbiome F/B ratio as exhaustive exercise after 6 weeks.

4.2 | Microbiome adaptations to PEMF and exercise interventions

A majority of the OTUs in the strenuously exercised cohort of mice, independent of PEMF treatment, pertained to the order *Bacteroidales*, dominated by the S24-7 family. This form of exercise by itself selected for gut bacteria involved in energy metabolism including S24-7, *Coriobacteriaceae spp*. and members of *Verrucomicrobia* and *Akkermansia spp*., previously shown to be inversely correlated with obesity, metabolic disorders, and inflammation.[92] *Akkermansia muciniphila* is a known butyrate (SCFA) producer that is associated with a lean body mass and improved metabolic health.[93,94] The gut microbiomes of PEMF-treated unexercised mice (–E/+P) were enriched in *Coriobacteriaceae spp*. and *Adlercreutzia* linked to lipid metabolism[95] and interscapular BAT thermogenesis and leanness in mice,[96] respectively. Thus, although 6 weeks of PEMF treatment alone was insufficient to achieve

beiging in WAT per se, the observed microbiome shifts were predictive of a leaner phenotype (lower F/B ratio) and exhibited correlations with greater thermogenic capacity.

By far, the most pronounced changes in muscle development and adipose thermogenesis were observed in the combined PEMF treatment and strenuously exercised (+E/+P) group. These mice showed enrichments of gut commensals including *Bacteroidales spp*., *Prevotella spp*., and *Ruminococcus spp*., which have been linked to improved energy metabolism in mice[97] and reduced incidence of weight gain in humans.[3] *Burkholderiales* was also enriched in this cohort and has been correlated with exercise adaptations in mice.[98] Here, we show that the microbial makeup of the strenuously exercised and PEMF-treated group (+E/+P) correlated with transcriptional upregulations indicative of adipose browning and thermogenesis (*Ucp1*), improved insulin-sensitivity (*Glut4*, *Irs1, Lep*) and mitochondriogenesis (*Cox7a1, Pgc-1α*) (Figure 3 and Table 3).

Exercise is an inflammatory stimulus that paves the way for physical and metabolic adaptations to oxidative stress,[99,100] a mitohormetic process[73,82,101] instigated by *Pgc-1α*.[102] Although the PEMF exposure paradigm used in the present report was relatively innocuous (60 minutes of total exposure distributed over 6 weeks at 1.5 mT) and previously provided no indications of cellular stress,[36] here, we combined it with an exercise regimen that was exhaustive by design, which in combination with PEMF treatment may have achieved a threshold level of inflammatory stress. The detection of *Proteus spp*., a pathobiont implicated in Inflammatory Bowel Disease[103] and *Coprobacillus spp*., implicated in gastrointestinal disease,[104] suggest that the combination of exhaustive exercise and weekly PEMF exposure (+E/+P) produced a level of oxidative stress not achieved in the exclusive exercised (+E/–P) or PEMF-treated (–E/+P) cohorts (Figure 2). For the dual intervention (+E/+P) cohort, an elevated level of inflammation may have produced a state of dysbiosis[105] manifested as a reduction in taxonomic diversity that may have enabled pathobionts to outcompete gut commensals, a process known as the competitive exclusion effect.[106] Conversely, the reduced diversity observed in the exclusive exercise (+E/–P) or PEMF-treated (–E/+P) cohorts may indicate microbiomal adaptations to enhance fidelity at the expense of diversity.[107] Further studies are required to resolve between these possibilities.

4.3 | Magnetic mitohormesis

We previously showed that PEMF exposure acts to instill mitochondrial survival adaptations associated with PGC-1α expression, a process of magnetically induced mitohormesis.[36] The data reported here would indicate that PEMF exposure is analogously inducing systemic mitohormesis in vivo. Muscular mitochondrial activation[82,101] and PGC-1α expression are recognized systemic mitohormesis inducers, mediated by PGC-1α/NRF/PPAR transcriptional coactivation of adaptive mitochondrial function.[57,71,73,82] These are genetic features shared by both exercise and the presented magnetic field intervention (Figures 1, 2, 4 and Tables 2, 3). The possibilities thus exist that magnetic field treatment may combine with concurrent exercise to either: (a) produce beneficial outcomes at low levels of cumulative mitochondrial activation or; (b) produce a restrictive inflammatory response resulting from excessively combined oxidative stresses; both these scenarios are in line with a mitohormetic mechanism and moreover, may represent different temporal stages of an ultimate unified adaptive response. In our 6-week exhaustive exercise study mice were exposed once per week (Sunday) and run to exhaustion thrice weekly on Mondays, Wednesdays, and Fridays. Running performance was generally slowest on Monday (greatest cumulative oxidative stress) and fastest on Friday (least cumulative oxidative stress), providing evidence of metabolically overwhelming interactions with greater temporal coincidence of the two interventions (Supplemental Figure S5); nonetheless, in the end the combination of PEMF exposure and exercise produced a greater level of physical adaptation. Microbiome and adipose measurements also produced signs of stressful systemic inflammation in mice undergoing both strenuous exercise and PEMF treatments (Figure 2B). Indeed, low levels of chronic stress have been shown to induce adipose browning in mice,[108] which aligns with the results reported for adipose tissues reported in this study. It is thus imperative that the timing of PEMF exposure as well as the level of exertion within the exercise regimen be adjusted to provide an optimal mitohormetic stimulus for positive adaptation, and moreover, may need to be intermittently gauged to match the basal level of inflammation of recipients as it changes during the course of the trial. Therefore, although the results represented in this report are consistent with the interpretation that PEMF exposure is inducing systemic mitohormetic adaptations, an analysis of the deeper systemic implications of our magnetic field exposure paradigm in animals and humans is warranted.

4.4 | Myokine response

CR (caloric restriction) browns and reduces adiposity, metabolic changes that are also correlated with alterations in the composition of the gut microbiota.[35] CR also stimulates muscular mitochondriogenesis and improves systemic insulin-sensitivity via the actions of SIRT1 and PGC-1α.[11,78,109] It is thus feasible that CR mediates its systemic effects largely by acting on the extensive muscular mitochondria pool. One manner in which the muscular mitochondrial pool would be capable of transmitting their response to the "system" is

via the release of myokines upon the activation of muscular mitochondrial respiration,[31-33,62,63] as PEMFs have been previously shown capable of doing.[36] Given that PEMF exposure[36] (Figures 1, 4), exercise,[23,51] and CR[11,78,109] all have in common that they activate SIRT1 and PGC-1α, similar myokine responses are likely to be elicited by any of the aforementioned interventions. Provocatively, myokines have been shown to induce the beiging of white adipose, ultimately stimulating its production and release of batokines, some of which are common to both cytokine pools and known as adipo-myokines[34,110] such as IGF-1 (Figure 1C), VEGFA (Figure S3E), adiponectin (Figure 4L), and IL-6 (Figure 4M), reinforcing the overall systemic response. The PEMF-induced mobilization of myokines and adipokines reported here hence supports such a physiological scheme. In further support of such a mechanism, it was recently shown that PEMF exposure augments the secretome response of MSCs to possess heightened anti-inflammatory and prochondrogenic properties.[111] Our future studies will focus on the PEMF-induced muscle and adipose secretome responses in animals and humans and their contributions to a greater systemic mitohormetic response.

4.5 | Functional profiles of PEMF- and exercise-conditioned gut microbiota

The microbiomes of the unexercised control cohort (–E/–P) did not show any significant associations to specific KEGG functions. By contrast, the microbiota of the unexercised, but PEMF-treated cohort (–E/+P) were better adapted for carbohydrate (mannose and fructose) and nucleotide (purine) metabolism as well as amino acid transport. Notably, this cohort also exhibited a microbiota that was particularly well suited for ketone body synthesis and metabolism (Figure S6), likely resulting from elevated mitochondrial fatty acid oxidation (Figure 1C,D), indicating that PEMF treatment per se is capable of altering gut microbiomes to better support metabolic flexibility (Figures 4I, S6). Moreover, ketone bodies have been proposed to act as signaling molecules to induce states of systemic mitohormesis[15,112] in association with the PGC-1α-NRF1/2-TFAM mitochondrial cascade (Figure 4). The exercised alone cohort (+E/–P), on the contrary, had greater representations from KEGG genes concerned with energy metabolism (oxidative phosphorylation) and metabolism of cofactors and vitamins (ubiquinone and terpenoid, biotin). Finally, the combined exercise and PEMF cohort (+E/+P) exhibited gut microbiomes that were functionally geared for the transport and exchange of glutamate and aspartate with the host. These amino acids are precursors in the synthesis of the SCFAs, known to modulate obesity[113] and recognized PPAR agonists targeted to muscle.[85] Notably, butyrate is known to induce PGC-1α gene expression in skeletal muscleand adipose tissue as well as stimulates free fatty acid oxidation,[17] aligning with the results presented in this study. Enterocytes also use glutamate and aspartate as an energy source during epithelial layer renewal and nutrient absorption.[114,115] Finally, glutamate is also thought to play a central role in the bidirectional communication system between the "microbiota-gut-brain axis" through modulation of glutamatergic receptor activity.[116]

4.6 | Extraneous contributing factors

The possibility that extraneous factors may have contributed to the results reported here cannot be discounted. To control for collateral effects attributed to mouse handling, both control and experimental mice were placed into the PEMF device for the same period of time (10 minutes), with the exception that control mice did not receive active fields. Notably, weight gain was sometimes seen in mice undergoing PEMF treatment, but was not consistently observed. One possibility is that the handling of mice may have been perceived as a form of stress. Stress is known to cause significant weight loss in several strains of mice.[117] Therefore, stress, in one form or another, may have contributed to the variability in weight gain we observed, particularly in studies where mice received multiple weekly exposures to PEMFs. Supplemental Figure S7 shows the observed weight changes for the longest and shortest duration studies included in this report, 6 months, single (Figure S7A) and thrice (Figure S7B) weekly exposure in the absence of exercise, and 6 weeks, single weekly PEMF exposure in combination with exercise (Figure S7C). Interestingly, weight gain in the once weekly exposed long-term cohort was not correlated with significant changes in food (Figure S7D) or water (Figure S7G) intake, whereas the thrice weekly exposed cohorts, not experiencing PEMF-induced changes in weight gain, did reveal a trend to increase food (Figure S7E) and water (Figure S7H) intake. On the other hand, increases and decreases in serum free fatty acids (FFA) (Figure S7J) and triglyceride (TG) (Figure S7M) levels, respectively, were observed in the long-term singly exposed mouse cohort, but not the thrice weekly exposed cohort (Figure S7K,N). In agreement, it has been reported that exercise training stimulates adipose TG hydrolysis to produce FFAs for release into the general circulation for use by muscle as an energy substrate,[118] reflecting our reported enhancement in fatty acid oxidation (Figure 1D). Accordingly, the Respiratory Exchange Ratio (RER) consistently showed a tendency to decrease with PEMF exposure in all mouse cohorts (Figure S7S-U; also *cf* Figure 1D). No correlation was observed between magnitude of weight gain and any of the measured parameters achieving statistical significance in the long-term study. Succinctly, weight gain was variable, likely subject to collateral as well as experimental variables

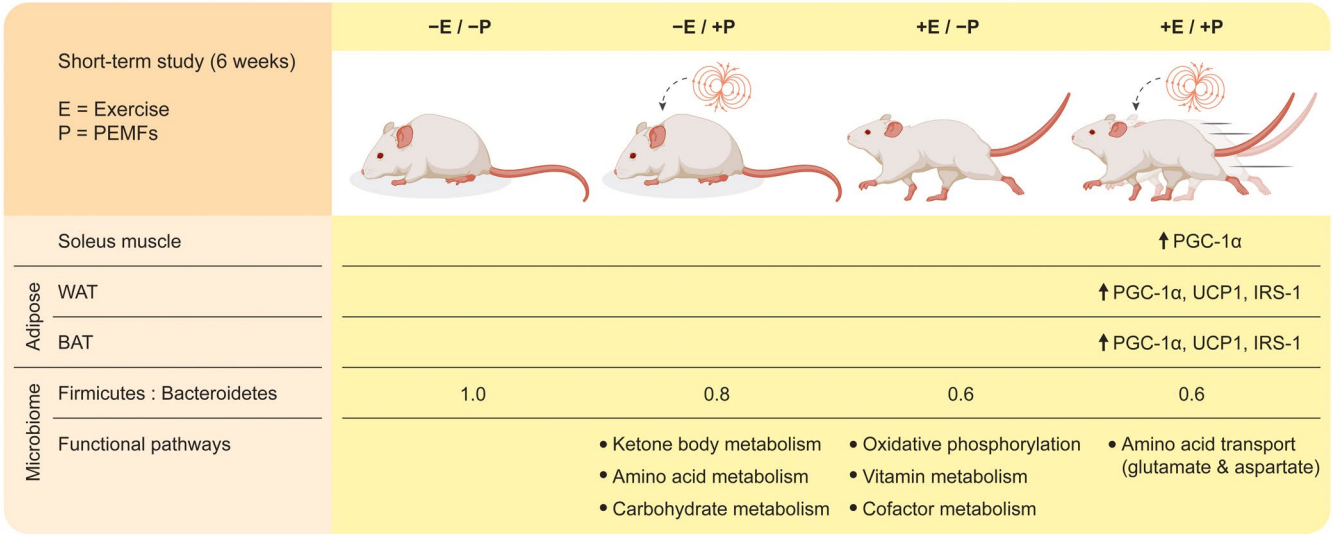

FIGURE 7 Graphical abstract for short-term exercise plus PEMF studies. The effects of PEMF exposure (1.5 mT, 10 min/week), with or without exhaustive exercise, during a 6-week trial conducted on four groups of mice: (1) no intervention; (2) PEMF treatment; (3) exercise; (4) exercise and PEMF treatment. Observed were significant upregulations of muscular and adipose *Pgc-1α* transcript levels, improved running capacity and indices of oxidative muscle development and adipose thermogenesis. Furthermore, the gut microbiome *Firmicutes/Bacteroidetes* ratio decreased incrementally between ascending groups. Beyond 8 weeks both PEMF exposure and exercise groups were individually capable of significantly raising *Pgc-1α* levels.

yet, not clearly correlated to any of the measured metabolic changes. The interactions between the duration and frequency of PEMF therapy with environmental stressors and consequently, with inherent stress responses, hence, require further studying. Handling-induced stress, however, would likely prove more consequential in small animal studies than in eventual human trials. Therefore, however provocative, these responses need to be confirmed with studies on larger cohorts of animals with greater number of independent variables with implemented controls for environmental stressors.

The results reported here indicate that PGC-1α is a common mediator of the metabolic effects of both exercise and PEMF treatment. In the short-term (≤6 weeks) a stronger statistical interaction was observed between *Pgc-1α* and related mitochondrial gene expressions with PEMF treatment, whereas adipose markers associated with insulin-sensitivity exhibited a stronger statistical interaction with exercise. Equally short-term PEMF treatment and exercise also produced unique shifts in microbiome communities and functional signatures with known associations to energy balance, while exhibiting low intragroup variability. Nonetheless, many key features previously associated with exercise-induced activation of PGC-1α were similarly evoked by PEMF treatment per se when administered for a few months including mitohormetic gene expression, oxidative muscle expression, enhanced mitochondrial fatty acid oxidation, systemic fatty acid oxidation, and insulin-sensitivity. We also revealed a novel association between magnetic field exposure and gut microbiome functional shifts toward metabolic improvement, implying a mutual link to PGC-1α. These metabolic responses, associated with PEMF exposure and/or exercise, despite being correlative, were internally consistent at several levels of physiological interaction and in agreement with published literature relating to the effects of muscle mitochondrial activation by exercise, as well as are in line with the predictions of our prior in vitro mechanistic studies showing PGC-1α upregulation in response to magnetic stimulation.[36] PEMF-based technologies hence may be ultimately exploited to complement, or accentuate, certain metabolic and physical attributes of exercise in humans unable to exercise because of illness, injury, or advanced age.

ACKNOWLEDGMENTS

We would like to acknowledge Professor Christian Wolfrum of the ETH Zürich, Department of Health Sciences and Technology for conducting the indirect calorimetry and blood analysis shown in Figure 1. We would also like to acknowledge Associate Professor Hyungwon Choi of the Department of Medicine of the NUS for helpful discussions on the statistical analytic methods employed in this study, particularly with reference to the utility and limitations of estimation plots used in Figures 2F,G, and S3.[43] Mr Zac Goh, iHealthtech (NUS) designed the graphical abstract shown in Figure 7. Financial support for this study was awarded from the Lee Foundation, Singapore (N-176-000-045-001), the Institute for Health Innovation & Technology, iHealthtech (R-176-000-243-731, Microbiome in Health, Disease and Ageing), at the National University of Singapore and the Ministry of Education Academic Research Fund (R-722-000-018-112 or MOE2018-T2-2-158). This study

was also partially funded by the European Space Agency Grant ESA-CORAGBF (4000113883) and the Fondation Suisse de Recherche sur les Maladies Musculaires.

CONFLICTS OF INTEREST

JF, CB, and AF-O. are inventors on patent WO 2019/17863 A1, System and Method for Applying Pulsed Electromagnetic Fields, and JF and AF-O. are contributors to QuantumTx Pte. Ltd., which elaborates electromagnetic field devices for human use. The other authors declare no conflicts of interest.

AUTHOR CONTRIBUTIONS

A. Franco-Obregón, Y. K. Tai, and C. Ng formulated the manuscript. K. Purnamawati, C. Wong, and B. K. Patel ran the short-term animal trials and CP Cerrato ran the long-term mouse trial. C. Ng, C. Wong, and B. K. Patel conducted the microbiome analysis. P. Pelczar designed and supervised the long-term mouse. A. Aguzzi and P. Pelczar conducted the muscle histology. A. Franco-Obregón, P. Pelczar, and K. Purnamawati conceived and designed the experiments. J. Fröhlich and C. Beyer designed and maintained the electromagnetic field apparatus used in this study. The remaining authors contributed in the form of data acquisition and analytics or in the support and mentoring of staff associated with the study. A. Franco-Obregón obtained funding for the project.

REFERENCES

1. Daniel H, Gholami AM, Berry D, et al. High-fat diet alters gut microbiota physiology in mice. *ISME J*. 2014;8:295-308.
2. Allen JM, Mailing LJ, Niemiro GM, et al. Exercise alters gut microbiota composition and function in lean and obese humans. *Med Sci Sport Exer*. 2018;50:747-757.
3. Menni C, Jackson MA, Pallister T, Steves CJ, Spector TD, Valdes AM. Gut microbiome diversity and high-fibre intake are related to lower long-term weight gain. *Int J Obes (2005)*. 2017;41:1099-1105.
4. Clavel T, Desmarchelier C, Haller D, et al. Intestinal microbiota in metabolic diseases: from bacterial community structure and functions to species of pathophysiological relevance. *Gut Microbes*. 2014;5:544-551.
5. Cani PD. Human gut microbiome: hopes, threats and promises. *Gut*. 2018;67:1716-1725.
6. Marchesi JR, Adams DH, Fava F, et al. The gut microbiota and host health: a new clinical frontier. *Gut*. 2016;65:330-339.
7. Gupta VK, Paul S, Dutta C. Geography, ethnicity or subsistence-specific variations in human microbiome composition and diversity. *Front Microbiol*. 2017;8:1162.
8. Fabbiano S, Suarez-Zamorano N, Chevalier C, et al. Functional gut microbiota remodeling contributes to the caloric restriction-induced metabolic improvements. *Cell Metab*. 2018;28:907–921.e7.
9. Wang S, Huang M, You X, et al. Gut microbiota mediates the anti-obesity effect of calorie restriction in mice. *Sci Rep*. 2018;8:13037.
10. Suarez-Zamorano N, Fabbiano S, Chevalier C, et al. Microbiota depletion promotes browning of white adipose tissue and reduces obesity. *Nat Med*. 2015;21:1497-1501.
11. Tang BL. Sirt1 and the mitochondria. *Mol Cells*. 2016;39:87-95.
12. Heiss CN, Olofsson LE. Gut microbiota-dependent modulation of energy metabolism. *J Innate Immun*. 2018;10:163-171.
13. Wicks SE, Vandanmagsar B, Haynie KR, et al. Impaired mitochondrial fat oxidation induces adaptive remodeling of muscle metabolism. *Proc Natl Acad Sci USA*. 2015;112:E3300-E3309.
14. Robinson MM, Dasari S, Konopka AR, et al. Enhanced protein translation underlies improved metabolic and physical adaptations to different exercise training modes in young and old humans. *Cell Metab*. 2017;25:581-592.
15. Mansueto G, Armani A, Viscomi C, et al. Transcription factor EB controls metabolic flexibility during exercise. *Cell Metab*. 2017;25:182-196.
16. Lahiri S, Kim H, Garcia-Perez I, et al. The gut microbiota influences skeletal muscle mass and function in mice. *Sci Transl Med*. 2019;11:5662.
17. Clark A, Mach N. The crosstalk between the gut microbiota and mitochondria during exercise. *Front Physiol*. 2017;8:319.
18. Cani PD, Van Hul M, Lefort C, Depommier C, Rastelli M, Everard A. Microbial regulation of organismal energy homeostasis. *Nat Metab*. 2019;1:34-46.
19. Houghton MJ, Kerimi A, Mouly V, Tumova S, Williamson G. Gut microbiome catabolites as novel modulators of muscle cell glucose metabolism. *FASEB J*. 2019;33:1887-1898.
20. Monda V, Villano I, Messina A, et al. Exercise modifies the gut microbiota with positive health effects. *Oxid Med Cell Longev*. 2017;2017:3831972.
21. Mach N, Fuster-Botella D. Endurance exercise and gut microbiota: a review. *J Sport Health Sci*. 2017;6:179-197.
22. Bressa C, Bailen-Andrino M, Perez-Santiago J, et al. Differences in gut microbiota profile between women with active lifestyle and sedentary women. *PLoS One*. 2017;12:e0171352.
23. Lin J, Wu H, Tarr PT, et al. Transcriptional co-activator PGC-1 alpha drives the formation of slow-twitch muscle fibres. *Nature*. 2002;418:797-801.
24. Cheng CF, Ku HC, Lin H. PGC-1alpha as a pivotal factor in lipid and metabolic regulation. *Int J Mol Sci*. 2018;19:3447.
25. Fraysse B, Desaphy JF, Pierno S, et al. Decrease in resting calcium and calcium entry associated with slow-to-fast transition in unloaded rat soleus muscle. *FASEB J*. 2003;17:1916-1918.
26. Xia L, Cheung KK, Yeung SS, Yeung EW. The involvement of transient receptor potential canonical type 1 in skeletal muscle regrowth after unloading-induced atrophy. *J Physiol*. 2016;594:3111-3126.
27. Zanou N, Schakman O, Louis P, et al. Trpc1 ion channel modulates phosphatidylinositol 3-Kinase/Akt pathway during myoblast differentiation and muscle regeneration. *J Biol Chem*. 2012;287:14524-14534.
28. Zanou N, Shapovalov G, Louis M, et al. Role of TRPC1 channel in skeletal muscle function. *Am J Physiol Cell Physiol*. 2010;298:C149-162.
29. Frey N, Frank D, Lippl S, et al. Calsarcin-2 deficiency increases exercise capacity in mice through calcineurin/NFAT activation. *J Clin Investig*. 2008;118:3598-3608.
30. Morales S, Diez A, Puyet A, et al. Calcium controls smooth muscle TRPC gene transcription via the camk/calcineurin-dependent pathways. *Am J Physiol Cell Physiol*. 2007;292:C553-C563.

31. Scheele C, Nielsen S, Pedersen BK. ROS and myokines promote muscle adaptation to exercise. *Trends Endocrin Met*. 2009;20:95-99.
32. Huh JY. The role of exercise-induced myokines in regulating metabolism. *Arch Pharm Res*. 2018;41:14-29.
33. Castillo-Quan JI. From white to brown fat through the PGC-1alpha-dependent myokine irisin: implications for diabetes and obesity. *Dis Model Mech*. 2012;5:293-295.
34. Villarroya F, Cereijo R, Villarroya J, Giralt M. Brown adipose tissue as a secretory organ. *Nat Rev Endocrinol*. 2017;13:26-35.
35. Li G, Xie C, Lu S, et al. Intermittent fasting promotes white adipose browning and decreases obesity by shaping the gut microbiota. *Cell Metab*. 2017;26:672-685 E674.
36. Yap JLY, Tai YK, Frohlich J, et al. Ambient and supplemental magnetic fields promote myogenesis via a TRPC1-mitochondrial axis: evidence of a magnetic mitohormetic mechanism. *FASEB J*. 2019;33:12853-12872.
37. Parate D, Franco-Obregon A, Frohlich J, et al. Enhancement of mesenchymal stem cell chondrogenesis with short-term low intensity pulsed electromagnetic fields. *Sci Rep*. 2017;7:9421.
38. Petrosino JM, Heiss VJ, Maurya SK, et al. Graded maximal exercise testing to assess mouse cardio-metabolic phenotypes. *PLoS One*. 2016;11:e0148010.
39. Kuczynski J, Stombaugh J, Walters WA, Gonzalez A, Caporaso JG, Knight R. Using QIIME to analyze 16S rRNA gene sequences from microbial communities. *Curr Protoc Bioinformatics*. 2011;36. Chapter 10, Unit 10 17.
40. Segata N, Izard J, Waldron L, et al. Metagenomic biomarker discovery and explanation. *Genome Biol*. 2011;12:R60.
41. Langille MG, Zaneveld J, Caporaso JG, et al. Predictive functional profiling of microbial communities using 16S Rrna marker gene sequences. *Nat Biotechnol*. 2013;31:814-821.
42. Clarke KR, Gorleya RN, Somerfield PJ, Warwick RM. *Change in Marine Communities: An Approach to Statistical Analysis and Interpretation*. 3rd ed. Plymouth: PRIMER-E Ltd; 2014.
43. Ho J, Tumkaya T, Aryal S, Choi H, Claridge-Chang A. Moving beyond P values: data analysis with estimation graphics. *Nat Methods*. 2019;16:565-566.
44. Van Wessel T, De Haan A, Van Der Laarse WJ, Jaspers RT. The muscle fiber type-fiber size paradox: hypertrophy or oxidative metabolism? *Eur J Appl Physiol*. 2010;110:665-694.
45. Ekmark M, Gronevik E, Schjerling P, Gundersen K. Myogenin induces higher oxidative capacity in pre-existing mouse muscle fibres after somatic DNA transfer. *J Physiol*. 2003;548:259-269.
46. Hudson MB, Price SR. Calcineurin: a poorly understood regulator of muscle mass. *Int J Biochem Cell Biol*. 2013;45:2173-2178.
47. Armand AS, Bourajjaj M, Martinez-Martinez S, et al. Cooperative synergy between NFAT and myod regulates myogenin expression and myogenesis. *J Biol Chem*. 2008;283:29004-29010.
48. Alfieri CM, Evans-Anderson HJ, Yutzey KE. Developmental regulation of the mouse IGF-I Exon 1 promoter region by calcineurin activation of NFAT in skeletal muscle. *Am J Physiol Cell Physiol*. 2007;292:C1887-C1894.
49. Crocetti S, Beyer C, Unternahrer S, et al. Impedance flow cytometry gauges proliferative capacity by detecting TRPC1 expression. *Cytometry*. 2014;85:525-536.
50. Supruniuk E, Miklosz A, Chabowski A. The implication Of PGC-1alpha on fatty acid transport across plasma and mitochondrial membranes in the insulin sensitive tissues. *Front Physiol*. 2017;8:923.
51. Lira VA, Benton CR, Yan Z, Bonen A. PGC-1alpha regulation by exercise training and its influences on muscle function and insulin sensitivity. *Am J Physiol Endocrinol Metab*. 2010;299:E145-E161.
52. Calvo JA, Daniels TG, Wang X, et al. Muscle-specific expression of Ppargamma coactivator-1alpha improves exercise performance and increases peak oxygen uptake. *J Appl Physiol (Bethesda, MD: 1985)*. 2008;104:1304-1312.
53. Henique C, Mansouri A, Vavrova E, et al. Increasing mitochondrial muscle fatty acid oxidation induces skeletal muscle remodeling toward an oxidative phenotype. *FASEB J*. 2015;29:2473-2483.
54. Tomiyama AJ. Stress and obesity. *Annu Rev Psychol*. 2019;70:703-718.
55. Kang C, Li Ji L. Role of PGC-1alpha signaling in skeletal muscle health and disease. *Ann N Y Acad Sci*. 2012;1271:110-117.
56. Roberts-Wilson TK, Reddy RN, Bailey JL, et al. Calcineurin signaling and PGC-1alpha expression are suppressed during muscle atrophy due to diabetes. *Biochem Biophys Acta*. 2010;1803:960-967.
57. Jung S, Kim K. Exercise-induced PGC-1alpha transcriptional factors in skeletal muscle. *Integr Med Res*. 2014;3:155-160.
58. Perroud J, Bernheim L, Frieden M, Koenig S. Distinct roles of Nfatc1 and Nfatc4 in human primary myoblast differentiation and in the maintenance of reserve cells. *J Cell Sci*. 2017;130:3083-3093.
59. Calabria E, Ciciliot S, Moretti I, et al. NFAT isoforms control activity-dependent muscle fiber type specification. *Proc Natl Acad Sci USA*. 2009;106:13335-13340.
60. Leick L, Hellsten Y, Fentz J, et al. PGC-1alpha mediates exercise-induced skeletal muscle VEGF expression in mice. *Am J Physiol Endocrinol Metab*. 2009;297:E92-E103.
61. Shin KO, Bae JY, Woo J, et al. The effect of exercise on expression of myokine and angiogenesis mRNA in skeletal muscle of high fat diet induced obese rat. *J Exerc Nutrition Biochem*. 2015;19:91-98.
62. Hoffmann C, Weigert C. Skeletal muscle as an endocrine organ: the role of myokines in exercise adaptations. *Cold Spring Harb Perspect Med*. 2017;7:a029793.
63. Lee JH, Jun HS. Role of myokines in regulating skeletal muscle mass and function. *Front Physiol*. 2019;10:42.
64. Pradhan RN, Zachara M, Deplancke B. A systems perspective on brown adipogenesis and metabolic activation. *Obes Rev*. 2017;18(Suppl 1):65-81.
65. Sepa-Kishi DM, Ceddia RB. Exercise-mediated effects on white and brown adipose tissue plasticity and metabolism. *Exerc Sport Sci Rev*. 2016;44:37-44.
66. Copps KD, White MF. Regulation of insulin sensitivity by serine/threonine phosphorylation of insulin receptor substrate proteins IRS1 And IRS2. *Diabetologia*. 2012;55:2565-2582.
67. Favaretto F, Milan G, Collin GB, et al. GLUT4 defects in adipose tissue are early signs of metabolic alterations in Alms1GT/GT, a mouse model for obesity and insulin resistance. *PLoS One*. 2014;9:e109540.
68. Matulewicz N, Stefanowicz M, Nikolajuk A, Karczewska-Kupczewska M. Markers of adipogenesis, but not inflammation, in adipose tissue are independently related to insulin sensitivity. *J Clin Endocrinol Metab*. 2017;102:3040-3049.
69. Motiani P, Virtanen KA, Motiani KK, et al. Decreased insulin-stimulated brown adipose tissue glucose uptake after

short-term exercise training in healthy middle-aged men. *Diabetes Obes Metab*. 2017;19:1379-1388.
70. Stromsdorfer KL, Yamaguchi S, Yoon MJ, et al. NAMPT-mediated NAD(+) biosynthesis in adipocytes regulates adipose tissue function and multi-organ insulin sensitivity in mice. *Cell Rep*. 2016;16:1851-1860.
71. Vargas-Mendoza N, Morales-Gonzalez A, Madrigal-Santillan EO, et al. Antioxidant and adaptative response mediated by Nrf2 during physical exercise. *Antioxidants (Basel)*. 2019;8:196.
72. Vina J, Gomez-Cabrera MC, Borras C, et al. Mitochondrial Biogenesis in exercise and in ageing. *Adv Drug Deliv Rev*. 2009;61:1369-1374.
73. Cox CS, Mckay SE, Holmbeck MA, et al. Mitohormesis in mice via sustained basal activation of mitochondrial and antioxidant signaling. *Cell Metab*. 2018;28:776–786.e5.
74. Erlich AT, Brownlee DM, Beyfuss K, Hood DA. Exercise induces TFEB expression and activity in skeletal muscle in a PGC-1alpha-dependent manner. *Am J Physiol Cell Physiol*. 2018;314:C62-C72.
75. Coleman V, Sa-Nguanmoo P, Koenig J, et al. Partial involvement of Nrf2 in skeletal muscle mitohormesis as an adaptive response to mitochondrial uncoupling. *Sci Rep*. 2018;8:2446.
76. Ross D, Siegel D. Functions of NQO1 in cellular protection and Coq10 metabolism and its potential role as a redox sensitive molecular switch. *Front Physiol*. 2017;8:595.
77. Mormeneo E, Jimenez-Mallebrera C, Palomer X, et al. PGC-1alpha induces mitochondrial and myokine transcriptional programs and lipid droplet and glycogen accumulation in cultured human skeletal muscle cells. *PLoS One*. 2012;7:E29985.
78. Morrow RM, Picard M, Derbeneva O, et al. Mitochondrial energy deficiency leads to hyperproliferation of skeletal muscle mitochondria and enhanced insulin sensitivity. *Proc Natl Acad Sci USA*. 2017;114:2705-2710.
79. Martinez-Huenchullan SF, Tam CS, Ban LA, Ehrenfeld-Slater P, Mclennan SV, Twigg SM. Skeletal muscle adiponectin induction in obesity and exercise. *Metabolism*. 2020;102:154008.
80. Fedewa MV, Hathaway ED, Ward-Ritacco CL, Williams TD, Dobbs WC. The effect of chronic exercise training on leptin: a systematic review and meta-analysis of randomized controlled trials. *Sports Med*. 2018;48:1437-1450.
81. Turnbaugh PJ, Ley RE, Mahowald MA, Magrini V, Mardis ER, Gordon JI. An obesity-associated gut microbiome with increased capacity for energy harvest. *Nature*. 2006;444:1027-1031.
82. Musci RV, Hamilton KL, Linden MA. Exercise-induced mitohormesis for the maintenance of skeletal muscle and healthspan extension. *Sports (Basel, Switzerland)*. 2019;7:170-188.
83. Allen JM, Berg Miller ME, Pence BD, et al. Voluntary and forced exercise differentially alters the gut microbiome in C57BL/6J mice. *J Appl Physiol (Bethesda, MD: 1985)*. 2015;118:1059-1066.
84. Petriz BA, Castro AP, Almeida JA, et al. Exercise induction of gut microbiota modifications in obese, non-obese and hypertensive rats. *BMC Genom*. 2014;15:511.
85. Oh HYP, Visvalingam V, Wahli W. The PPAR-microbiota-metabolic organ trilogy to fine-tune physiology. *FASEB J*. 2019;33:9706-9730. https://doi.org/10.1096/fj.201802681RR.
86. Mottawea W, Chiang CK, Muhlbauer M, et al. Altered intestinal microbiota-host mitochondria crosstalk in new onset Crohn's disease. *Nat Commun*. 2016;7:13419.
87. Saint-Georges-Chaumet Y, Edeas M. Microbiota-mitochondria inter-talk: consequence for microbiota-host interaction. *Pathog Dis*. 2016;74:ftv096. https://doi.org/10.1093/femspd/ftv096.
88. De Las Heras N, Klett-Mingo M, Ballesteros S, et al. Chronic exercise improves mitochondrial function and insulin sensitivity in brown adipose tissue. *Front Physiol*. 2018;9:1122.
89. Bernlohr DA. Exercise and mitochondrial function in adipose biology: all roads lead to NO. *Diabetes*. 2014;63:2606-2608.
90. Ley RE, Backhed F, Turnbaugh P, Lozupone CA, Knight RD, Gordon JI. Obesity alters gut microbial ecology. *Proc Natl Acad Sci USA*. 2005;102:11070-11075.
91. Ley RE, Turnbaugh PJ, Klein S, Gordon JI. Microbial ecology: human gut microbes associated with obesity. *Nature*. 2006;444:1022-1023.
92. Cani PD, De Vos WM. Next-generation beneficial microbes: the case of *Akkermansia muciniphila*. *Front Microbiol*. 2017;8:1765.
93. Dao MC, Everard A, Aron-Wisnewsky J, et al. *Akkermansia muciniphila* and improved metabolic health during a dietary intervention in obesity: relationship with gut microbiome richness and ecology. *Gut*. 2016;65:426-436.
94. Louis P, Flint HJ. Diversity, metabolism and microbial ecology of butyrate-producing bacteria from the human large intestine. *FEMS Microbiol Lett*. 2009;294:1-8.
95. Martinez I, Perdicaro DJ, Brown AW, et al. Diet-induced alterations of host cholesterol metabolism are likely to affect the gut microbiota composition in hamsters. *Appl Environ Microbiol*. 2013;79:516-524.
96. Zietak M, Kovatcheva-Datchary P, Markiewicz LH, Stahlman M, Kozak LP, Backhed F. Altered microbiota contributes to reduced diet-induced obesity upon cold exposure. *Cell Metab*. 2016;23:1216-1223.
97. Ravussin Y, Koren O, Spor A, et al. Responses of gut microbiota to diet composition and weight loss in lean and obese mice. *Obesity (Silver Spring, MD)*. 2012;20:738-747.
98. Liu Z, Liu HY, Zhou H, et al. Moderate-intensity exercise affects gut microbiome composition and influences cardiac function in myocardial infarction mice. *Front Microbiol*. 2017;8:1687.
99. Brown WM, Davison GW, Mcclean CM, Murphy MH. A systematic review of the acute effects of exercise on immune and inflammatory indices in untrained adults. *Sports Med Open*. 2015;1:35.
100. Sloan RP, Shapiro PA, Mckinley PS, et al. Aerobic exercise training and inducible inflammation: results of a randomized controlled trial in healthy, young adults. *J Am Heart Assoc*. 2018;7:E010201.
101. Ristow M, Schmeisser K. Mitohormesis: promoting health and lifespan by increased levels of reactive oxygen species (ROS). *Dose-Response*. 2014;12:288-341.
102. Handschin C, Spiegelman BM. The role of exercise and PGC1alpha in inflammation and chronic disease. *Nature*. 2008;454:463-469.
103. Forbes JD, Van Domselaar G, Bernstein CN. The gut microbiota in immune-mediated inflammatory diseases. *Front Microbiol*. 2016;7:1081.
104. Pontarelli EM, Ford HR, Gayer CP. Recent developments in Hirschsprung's-associated enterocolitis. *Curr Gastroenterol Rep*. 2013;15:340.
105. Pham TA, Lawley TD. Emerging insights on intestinal dysbiosis during bacterial infections. *Curr Opin Microbiol*. 2014;17:67-74.
106. Bull MJ, Plummer NT. Part 1: the human gut microbiome in health and disease. *Integr Med (Encinitas, Calif.)*. 2014;13:17-22.

107. Reese AT, Dunn RR. Drivers of microbiome biodiversity: a review of general rules, feces, and ignorance. *mBio*. 2018;9:E01294-01218.
108. Razzoli M, Frontini A, Gurney A, et al. Stress-induced activation of brown adipose tissue prevents obesity in conditions of low adaptive thermogenesis. *Mol Metab*. 2016;5:19-33.
109. Weir HJ, Yao P, Huynh FK, et al. Dietary restriction and AMPK increase lifespan via mitochondrial network and peroxisome remodeling. *Cell Metab*. 2017;26:884-896.e5.
110. Graf C, Ferrari N. Metabolic health—the role of adipo-myokines. *Int J Mol Sci*. 2019;20:6159.
111. Parate D, Kadir ND, Celik C, et al. Pulsed electromagnetic fields potentiate the paracrine function of mesenchymal stem cells for cartilage regeneration. *Stem Cell Res Ther*. 2020;11:46.
112. Miller VJ, Villamena FA, Volek JS. Nutritional ketosis and mitohormesis: potential implications for mitochondrial function and human health. *J Nutr Metab*. 2018;2018:5157645.
113. Neis EP, Dejong CH, Rensen SS. The role of microbial amino acid metabolism in host metabolism. *Nutrients*. 2015;7:2930-2946.
114. Blachier F, Boutry C, Bos C, Tome D. Metabolism and functions of L-glutamate in the epithelial cells of the small and large intestines. *Am J Clin Nutr*. 2009;90:814s-821s.
115. Watford M, Lund P, Krebs HA. Isolation and metabolic characteristics of rat and chicken enterocytes. *Biochem J*. 1979;178:589-596.
116. Baj A, Moro E, Bistoletti M, Orlandi V, Crema F, Giaroni C. Glutamatergic signaling along the microbiota-gut-brain axis. *Int J Mol Sci*. 2019;20:1482. https://doi.org/10.3390/ijms20061482.
117. Mozhui K, Karlsson RM, Kash TL, et al. Strain differences in stress responsivity are associated with divergent amygdala gene expression and glutamate-mediated neuronal excitability. *J Neurosci*. 2010;30:5357-5367.
118. Mika A, Macaluso F, Barone R, Di Felice V, Sledzinski T. Effect of exercise on fatty acid metabolism and adipokine secretion in adipose tissue. *Front Physiol*. 2019;10:26.

SUPPORTING INFORMATION

Additional Supporting Information may be found online in the Supporting Information section.

How to cite this article: Tai YK, Ng C, Purnamawati K, et al. Magnetic fields modulate metabolism and gut microbiome in correlation with *Pgc-1α* expression: Follow-up to an in vitro magnetic mitohormetic study. *The FASEB Journal*. 2020;34:11143–11167. https://doi.org/10.1096/fj.201903005RR